ornl

ORNL/TM-10164

MARTIN MARIETTA ENERGY SYSTEMS LIBRARIES

3 4456 0278641 1

OAK RIDGE NATIONAL LABORATORY

MARTIN MARIETTA

Modular Pump Limiter Systems for Large Tokamaks

T. Uckan
C. C. Klepper
P. K. Mioduszewski
R. T. McGrath

OAK RIDGE NATIONAL LABORATORY
CENTRAL RESEARCH LIBRARY
CIRCULATION SECTION
4500N ROOM 175
LIBRARY LOAN COPY
DO NOT TRANSFER TO ANOTHER PERSON
If you wish someone else to see this report, send in name with report and the library will arrange a loan.

OPERATED BY
MARTIN MARIETTA ENERGY SYSTEMS, INC.
FOR THE UNITED STATES
DEPARTMENT OF ENERGY

Printed in the United States of America. Available from
National Technical Information Service
U.S. Department of Commerce
5285 Port Royal Road, Springfield, Virginia 22161
NTIS price codes—Printed Copy: A04; Microfiche A01

This report was prepared as an account of work sponsored by an agency of the United States Government. Neither the United States Government nor any agency thereof, nor any of their employees, makes any warranty, express or implied, or assumes any legal liability or responsibility for the accuracy, completeness, or usefulness of any information, apparatus, product, or process disclosed, or represents that its use would not infringe privately owned rights. Reference herein to any specific commercial product, process, or service by trade name, trademark, manufacturer, or otherwise, does not necessarily constitute or imply its endorsement, recommendation, or favoring by the United States Government or any agency thereof. The views and opinions of authors expressed herein do not necessarily state or reflect those of the United States Government or any agency thereof.

ORNL/TM-10164
Dist. Category UC-20 a,d,f

Fusion Energy Division

MODULAR PUMP LIMITER SYSTEMS FOR LARGE TOKAMAKS

T. Uckan
C. C. Klepper
P. K. Mioduszewski

R. T. McGrath
Sandia National Laboratories, Albuquerque, New Mexico 87175

Date Published - September 1987

Prepared by the
OAK RIDGE NATIONAL LABORATORY
Oak Ridge, Tennessee 37830
operated by
MARTIN MARIETTA ENERGY SYSTEMS, INC.
for the
U.S. DEPARTMENT OF ENERGY
under contract DE-AC05-84OR21400

MARTIN MARIETTA ENERGY SYSTEMS LIBRARIES
3 4456 0278641 1

CONTENTS

ABSTRACT v

I. INTRODUCTION 1

II. MODULAR PUMP LIMITER 3

A. Particle Exhaust of a Modular Pump Limiter 4

B. Power Removal with a Modular Pump Limiter 8

C. SOL Plasma Characteristics 9

III. MODULAR PUMP LIMITER SYSTEM 11

A. Pump Limiter System Particle Exhaust 11

B. Location of Pump Limiter Modules and Shadowing Considerations 13

IV. TORE SUPRA PUMP LIMITER SYSTEM 19

V. EFFECTS OF MAGNETIC FIELD RIPPLE ON THE LIMITER MODULE 25

VI. DISCUSSIONS 29

ACKNOWLEDGMENTS 31

REFERENCES 33

Appendix A: Calculation of Q_n(max) for a Circular Cooling Channel . . 35

Appendix B: Parameters of SOL Plasma 35

ABSTRACT

Long-pulse (>10-s) operation of large tokamaks with high-power (>10-MW) heating and extensive external fueling will require correspondingly efficient particle exhaust for density control. A pump limiter can provide the needed exhaust capability by removing a small percentage of the particles, which would otherwise be recycled. Single pump limiter modules have been operated successfully on ISX-B, PDX, TEXTOR, and PLT. An axisymmetric pump limiter is now being installed and will be studied in TEXTOR. A third type of pump limiter is a system that consists of several modules and exhibits performance different from that of a single module. To take advantage of the flexibility of a modular pump limiter system in a high-power, long-pulse device, the power load must be distributed among a number of modules. Because each added module changes the performance of all the others, a set of design criteria must be defined for the overall limiter system. The design parameters for the modules are then determined from the system requirements for particle and power removal. Design criteria and parameters are presented, and the impact on module design of the state of the art in engineering technology is discussed. The relationships between modules are considered from the standpoint of flux coverage and shadowing effects. The results are applied to the Tore Supra tokamak. A preliminary conceptual design for the Tore Supra pump limiter system is discussed, and the design parameters of the limiter modules are presented.

I. INTRODUCTION

Long-pulse (>10-s) operation of large tokamaks with high-power (>10-MW) heating and extensive external fueling requires efficient techniques for particle and power removal. One possible solution, as planned for the Tore Supra tokamak,[1] is to use a pump limiter system. A pump limiter can provide the exhaust capability needed for density control by removing a small percentage of the particles, which would otherwise be recycled. Single pump limiter modules have been operated successfully on the Impurity Study Experiment (ISX-B),[2] the Poloidal Divertor Experiment (PDX),[3] TEXTOR,[4] and the Princeton Large Torus (PLT).[5] An axisymmetric pump limiter is now being installed on TEXTOR[6] and will be operated in late 1987. A third type of pump limiter is a system that consists of several modules and exhibits performance different from that of a single module. To take advantage of the flexibility of a modular pump limiter system in a high-power, long-pulse device, the power load must be distributed among a number of modules. Since each added module changes the performance of all the others, design criteria must be defined for the overall limiter system and then applied to module design. The relationship between individual modules must also be considered from the standpoint of flux coverage and shadowing effects.

For long-pulse or steady-state operation, the limiter modules must be equipped with active cooling. At the leading edge of the module, the cooling channel determines the thickness of the limiter blade (or head). The design of a pump limiter module is always a compromise between a thin blade for high particle exhaust and a leading edge that is sufficiently recessed to be in a region of tolerable heat flux. We have developed a model for estimating the system exhaust efficiency in terms of the parameters of the limiter leading edge (i.e., its thickness and the design heat flux) for given device parameters and the power load that must be removed.

In order to estimate the exhaust efficiency for controlling the core plasma density N_e for a given tokamak, we use the global particle balance relation:

$$\frac{dN_e}{dt} = \phi_{ext} + \frac{N_e}{\bar{\tau}_p}(\bar{R} - 1) - \phi_{exh}(\mathrm{PL}) \quad , \tag{1}$$

where ϕ_{ext}, $\phi_{exh}(\mathrm{PL})$, $\bar{\tau}_p$, and $\bar{R}$ are the external fueling rate, the particle exhaust rate provided by the pump limiters, the global particle confinement time, and the global recycling coefficient, respectively. The recycling coefficient is the ratio of the total recycled particle flux (from the limiters and wall) and the total incident flux; its value can reach $\bar{R} \simeq 1$ within a few seconds of the plasma discharge for long-pulse

operation of a tokamak. Therefore, as we see from Eq. (1), for particle equilibrium, the external fueling [from, for example, gas puff, neutral beam injection (NBI), and pellets] must be balanced by the particle exhaust provided by the pump limiters in the system; that is, $\phi_{\rm ext} = \phi_{\rm exh}({\rm PL})$. Since $\phi_{\rm exh}({\rm PL})$ is a given fraction ϵ of the total particle efflux, $N_{\rm e}/\bar{\tau}_p$, we can estimate the required pump limiter system exhaust efficiency as

$$\epsilon = \frac{\phi_{\rm ext}}{N_{\rm e}/\bar{\tau}_p} \quad , \tag{2}$$

from the total fueling rate $\phi_{\rm ext} = \phi_{\rm gas\ puff} + \phi_{\rm NBI} + \phi_{\rm pellets}$. Using Eq. (2) in Eq. (1), we also get the equilibrium plasma density,

$$N_{\rm e} = \frac{\phi_{\rm ext}\bar{\tau}_p}{1 - \bar{R}_{\rm eff}} \quad , \tag{3}$$

where $\bar{R}_{\rm eff} = \bar{R} - \epsilon$ is the effective recycling coefficient with the pump limiters.

Equation (3) demonstrates that the plasma density can be controlled very effectively using pump limiters with a relatively low exhaust efficiency ($\epsilon \sim 0.1$) provided $\bar{R} \simeq 1$, which is the case for long-pulse tokamaks. It also shows that pump limiters reduce the global recycling by a small fraction, which is the basic principle of their operation (see Refs. 7 and 8 for details). The goal of this paper is to discuss criteria for the optimization of particle exhaust as a function of heat loads and then to apply these criteria to study the performance of a system of modular pump limiters. To do this, we first briefly review the characteristics of a modular pump limiter and then proceed to study a pump limiter system for large tokamaks.

In Section II, we discuss the basic properties of a modular pump limiter for particle and power removal. In Section III, we apply these properties to the design of a system with several modules and discuss the relationships among modules and their implications for particle and power removal. We develop a model for estimating the system exhaust efficiency in terms of the parameters of the actively cooled leading edge. The choice of locations for the modules is also discussed, and the effects of shadowing between modules on particle and power removal are examined. In Section IV, the formulation discussed in Section III is used to estimate the design parameters for the Tore Supra[1] pump limiter system, and overall system characteristics are presented. The effects of magnetic field ripple on the limiter design are briefly examined in Section V. General remarks and discussions are contained in Section VI.

II. MODULAR PUMP LIMITER

In this section, we review the characteristics of a typical modular pump limiter with an actively cooled leading edge that can remove 2–3 kW/cm^2 from a tokamak plasma, as shown in Fig. 1. These characteristics are then used to explore the relationships between N combined modules.

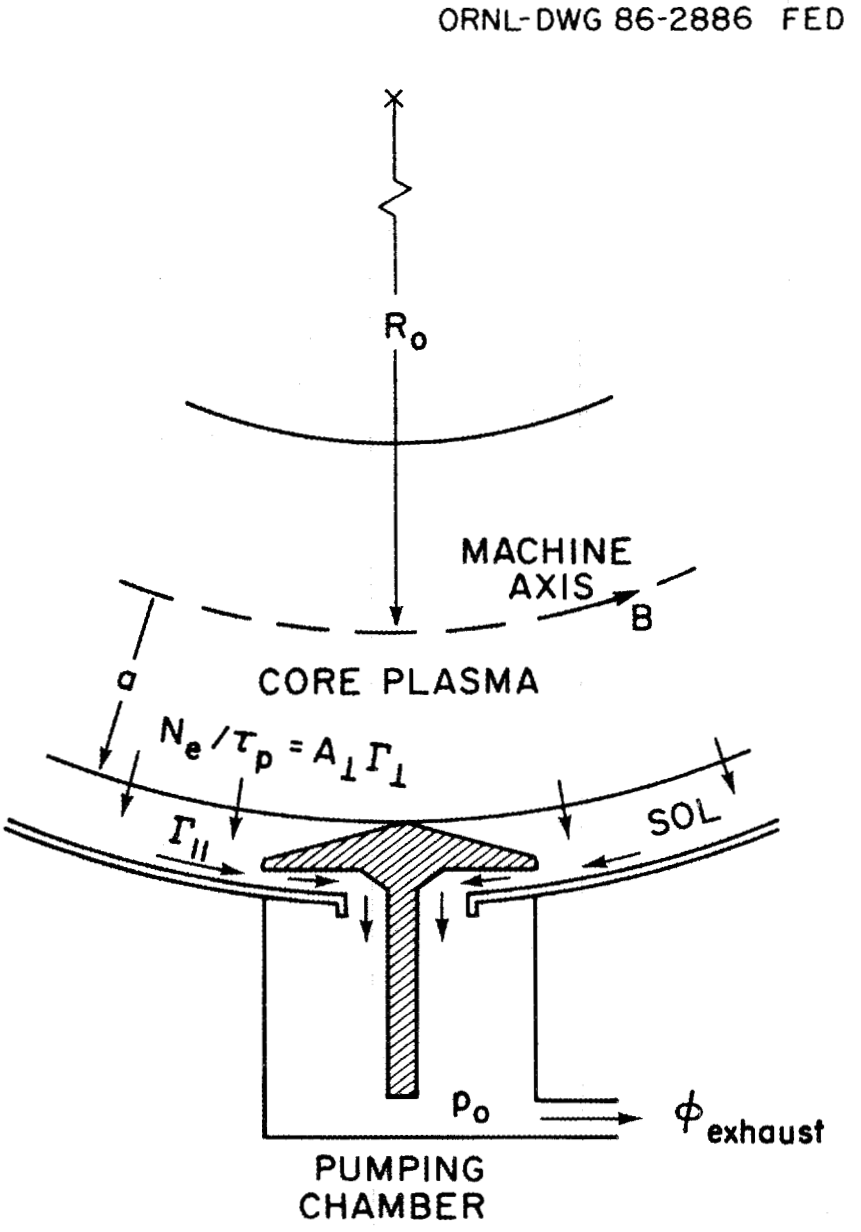

Fig. 1. Typical pump limiter in a tokamak. A fraction of the core plasma particles is captured by the limiter; after neutralization, these particles are pumped out of the device.

A. Particle Exhaust of a Modular Pump Limiter

A typical modular pump limiter and its parameters are shown schematically in Fig. 2. Particles are assumed to enter the pump limiter from both the ion and the electron sides. In the figure, the x-coordinate is the distance into the scrape-off layer (SOL) plasma from the last closed flux surface, which is defined by the location of the pump limiter head in the tokamak, as shown in Fig. 2(b). The dimensions of the module head are L_θ in the poloidal direction and L_ϕ in the toroidal direction;

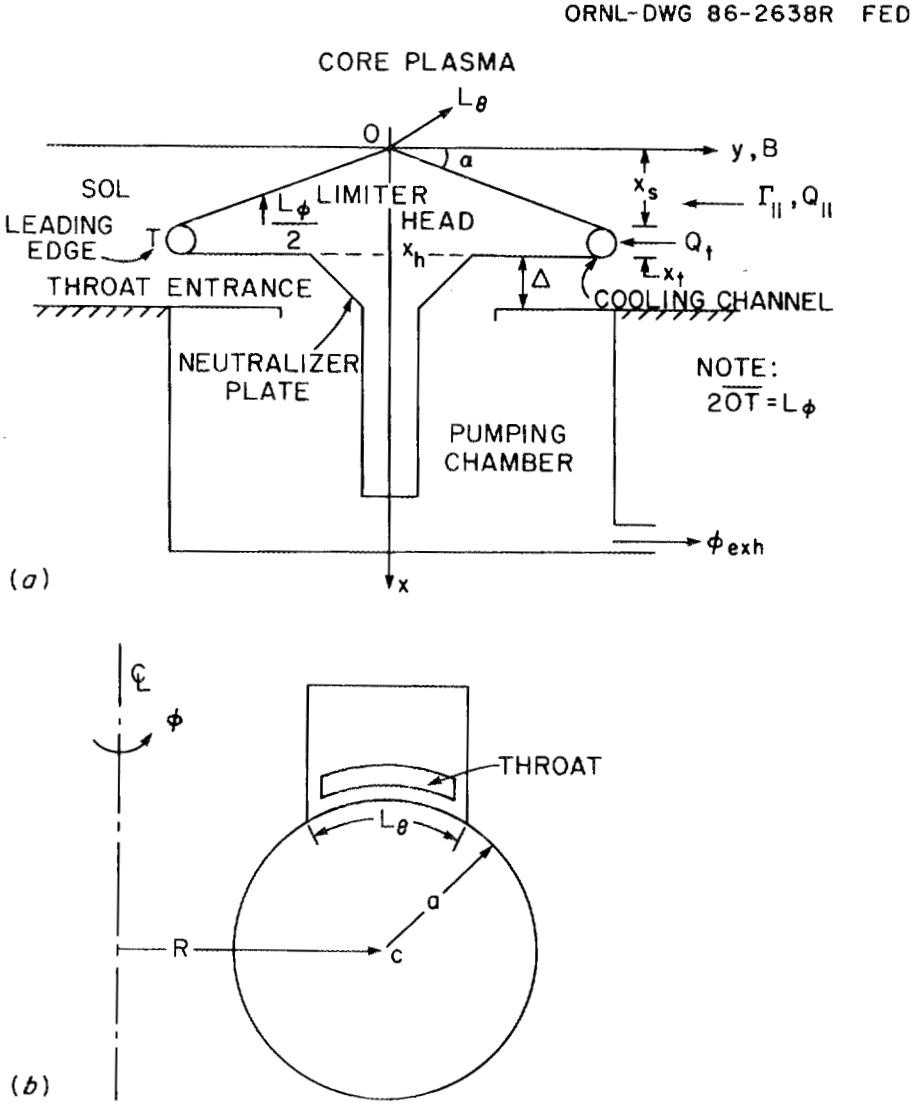

Fig. 2. (a) Schematic of a typical modular pump limiter and its characteristic parameters. (b) Location of the module in the tokamak plasma.

x_h is the module head thickness, x_t is the diameter of the cooling channel on the leading edges (tips) of the module, and Δ is the throat entrance width.

The particle exhaust efficiency of a pump limiter module ϵ_{PL}, which indicates the fraction of the total plasma efflux $\phi_{plasma} = N_e/\bar{\tau}_p$ that is pumped out of the device, is

$$\epsilon_{PL} = \frac{\phi_{exh}}{\phi_{plasma}} \quad . \tag{4}$$

Equation (4) can also be expressed in terms of the various fractions of the particle flux defined by the module:

$$\epsilon_{PL} = \left(\frac{\phi_{module}}{\phi_{plasma}}\right)\left(\frac{\phi_{throat}}{\phi_{module}}\right)\left(\frac{\phi_{exh}}{\phi_{throat}}\right) \ ,$$

where ϕ_{module} is the total flux available to the module for exhaust and ϕ_{throat} is the total particle flux in the throat entrance of the module. Each fraction in this expression for ϵ_{PL} may be viewed as one of the characteristic efficiencies of the module. That is,

$$\epsilon_{PL} = \epsilon_{MC} \times \epsilon_{coll} \times \epsilon_R \quad , \tag{5}$$

where ϵ_{MC}, ϵ_{coll}, and ϵ_R are the module coverage, collection, and particle removal efficiencies, respectively. We briefly discuss these efficiencies.

1. Module coverage

For simplicity, we ignore the toroidal effects and assume a cylindrical geometry in poloidal (θ) and toroidal (ϕ) space for the last closed flux surface, where the modular pump limiter is located. As shown in Fig. 3, the module defines a flux tube through which the SOL particles flow and become available to the module for exhaust. In this configuration, the pump limiter has a poloidal extent $\theta_L = L_\theta/a$ and a toroidal extent $\phi_L = L_\phi/R$; here a is the radial location of the limiter, and $R = R_0 + a\cos\theta$, where R_0 is the major radius of the device. We also define a poloidal module flux coverage angle θ_{MC}, indicated in Fig. 3 and given by

$$\theta_{MC} = \theta_L - \phi_L/q \ , \tag{6}$$

where $q \equiv q(a)$ is the edge safety factor.

As we see from Fig. 3, at the plasma boundary, $x = 0$, the pump limiter module intercepts only a fraction of the total particle efflux, $N_e/\bar{\tau}_p = \Gamma_\perp(0)A_\perp = \Gamma_\perp(0) \times 2\pi a \times 2\pi R_0$, where $\Gamma_\perp(0)$ is the outward particle flux at the limiter location. Therefore, the total flux available to the module for q toroidal revolutions is

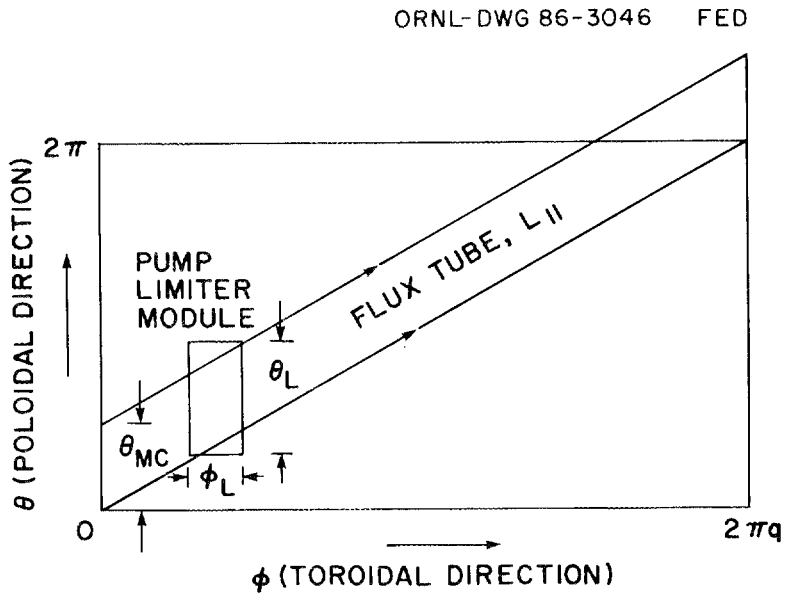

Fig. 3. Pump limiter in (θ, ϕ) space. The module defines a flux tube through which particles in the SOL flow into the module throat entrance for pumping out of the system.

given by $\phi_{\text{module}} = \Gamma_\perp(0) A_\perp(M)$, where $A_\perp(M) = (a \times \theta_{\text{MC}}) \times L_\parallel$ is the module flux tube area shown in the figure, defined along the magnetic field line with an average length of $L_\parallel = 2\pi q R_0$. The module coverage then becomes

$$\epsilon_{\text{MC}} = \frac{A_\perp(M)}{A_\perp} = \left(\frac{\theta_{\text{MC}}}{2\pi}\right)\left(\frac{L_\parallel}{2\pi R_0}\right) , \tag{7}$$

and by using Eq. (6) in ϵ_{MC}, we find

$$\epsilon_{\text{MC}} \simeq q L_\theta / 2\pi a \quad . \tag{8}$$

Here we have made use of the fact that $\theta_{\text{L}} > \phi_{\text{L}}$.

2. Particle collection efficiency

We begin our discussion of the particle collection efficiency with the particles in the SOL plasma. Some of these particles enter the pump limiter throat (Th); this particle flux is given by

$$\phi_{\text{throat}} = \int_{\text{Th}} dA \; \Gamma_\parallel(x) \; , \tag{9}$$

where $\int_{\mathrm{Th}} dA = 2L_\theta\Delta$ is the area of the module throat entrance and $\Gamma_{\|}(x) = \Gamma_{\|}(0)\exp(-x/\lambda_\Gamma)$ is the flux along the magnetic field in the SOL, which has a characteristic scale length of λ_Γ. The total flux available for the module is

$$\phi_{\mathrm{module}} = \Gamma_\perp(0)A_\perp(M) = 2L_\theta \int_0^\infty dx\Gamma_{\|}(x) = \Gamma_{\|}(0)A_{\|}(M) \ ,$$

where $A_{\|}(M) = 2L_\theta\lambda_\Gamma$. We carry out the integration in Eq. (9) from $x = x_{\mathrm{h}}$ to $x_{\mathrm{h}} + \Delta$ and obtain

$$\epsilon_{\mathrm{coll}} = \frac{\phi_{\mathrm{throat}}}{\phi_{\mathrm{module}}} = \exp(-x_{\mathrm{h}}/\lambda_\Gamma)[1 - \exp(-\Delta/\lambda_\Gamma)] \ . \tag{10}$$

The throat entrance width Δ should be at least a particle density scale length λ_n of the SOL for a high value of ϵ_{coll}.[7] However, if Δ is too large, then the particle backflow is high and the pressure buildup needed for good pumping cannot be established.

3. Particle removal efficiency

As noted in Section II.A.1, only some of the particles in the SOL enter the module throat and have a chance to be exhausted out of the pumping chamber. Some of these particles leave the module and go back to the SOL (backflow); some of them hit the neutralizer plate and then scatter into the module pumping chamber. The scattered neutral particles build up pressure in the pumping chamber until the sum of the backflow out of the chamber and the particle flux actually removed by pumping ϕ_{exh} becomes equal to ϕ_{throat}. As defined earlier, the particle removal efficiency ϵ_{R}, the part of ϕ_{throat} that is actually removed by pumping, is

$$\epsilon_{\mathrm{R}} = \phi_{\mathrm{exh}}/\phi_{\mathrm{throat}} \ . \tag{11}$$

The particle exhaust ϕ_{exh} out of the pump limiter module can be calculated from the pressure buildup p_0 in the pumping chamber and the effective pumping speed S_{eff} of the module pump:

$$\phi_{\mathrm{exh}} = p_0 \times S_{\mathrm{eff}} \ . \tag{12}$$

Recent experiments with ALT-I[9,10] on TEXTOR indicate that the removal efficiency of a modular pump limiter is around 60 to 70%. For our calculations, we assume that $\epsilon_{\mathrm{R}} = 70\%$.

As discussed in Section III, the limiter throat can be shadowed if there are multiple modules in the system. This may set up regions of different plasma densities, or "stripes," in the entrance channel, which would affect the particle removal efficiency. This effect is ignored here, but it should be investigated.

B. Power Removal with a Modular Pump Limiter

The total power received by the modular pump limiter $P_{\rm L}$ is the sum of the power to the limiter surface $P_{\rm s}$, the power to the leading edge $P_{\rm t}$, and the power to the neutralizer plate $P_{\rm n}$. The heat flux profile of the SOL,

$$Q_{\|}(x) = Q_0 \exp(-x/\lambda_q) \ , \tag{13}$$

where λ_q is the scale length and $Q_0 \equiv Q_{\|}(x=0)$ at the boundary, can be used to write the components of the total power:

$$P_{\rm s} = 2L_\theta \int_0^{x_{\rm s}} dx\ Q_{\|}(x) = 2L_\theta Q_0 \lambda_q \left[1 - \exp(-x_{\rm s}/\lambda_q)\right] \ , \tag{14}$$

$$P_{\rm t} = 2L_\theta \int_{x_{\rm s}}^{x_{\rm s}+x_{\rm t}} dx\ Q_{\|}(x) = 2L_\theta Q_0 \lambda_q \exp(-x_{\rm s}/\lambda_q) \left[1 - \exp(-x_{\rm t}/\lambda_q)\right] \ , \tag{15}$$

and

$$P_{\rm n} = 2L_\theta Q_0 \lambda_q \exp(-x_{\rm h}/\lambda_q)\ \left[1 - \exp(-\Delta/\lambda_q)\right] \ . \tag{16}$$

From Eqs. (14)–(16),

$$P_{\rm L} = 2L_\theta Q_0 \lambda_q \{1 - \exp[-(x_{\rm h} + \Delta)/\lambda_q]\} \ . \tag{17}$$

Note that $x_{\rm h} = x_{\rm t} + x_{\rm s}$. The limiter power $P_{\rm L}$ is a fraction of the total heating power of the tokamak; typically

$$P_{\rm L} = (0.5\text{–}0.8) \times P_{\rm heating} \ . \tag{18}$$

This must be assumed to be a known parameter for a modular pump limiter design.

The heat fluxes on the surfaces of the limiter at $x = 0$ and of the leading-edge cooling channel (as discussed in Appendix A), where $x = x_{\rm h} - x_{\rm t}/2$, must be below their design values of $Q_{\rm d}$ and $Q_{\rm t}$:

$$Q_{\rm n} = Q_{\|}(0) \sin\alpha \le Q_{\rm d} \tag{19}$$

and

$$Q_{\|}(x_{\rm h} - x_{\rm t}/2) = Q_0 \exp[-(x_{\rm h} - x_{\rm t}/2)/\lambda_q] \le Q_{\rm t} \ , \tag{20}$$

where Q_n is the heat flux normal to the limiter surface at $x = 0$ and α is the angle between the limiter surface and the magnetic field (or the particle flow), as shown in Fig. 2(a). With present engineering technology,[11] for example in the case of Tore Supra's limiter modules, typical design heat flux values are[12] $Q_d \simeq 300$–500 W/cm^2 and $Q_t \simeq 3$ kW/cm^2. It is clear that for large tokamaks with $P_{\text{heating}} \geq 10$ MW, more than one modular pump limiter is required just to handle the power.

C. SOL Plasma Characteristics

In order to estimate the particle exhaust and power removal of the modular pump limiter, we need to know the characteristics of the SOL plasma, including the scale lengths of the particle and heat fluxes. These lengths, λ_Γ and λ_q, may be estimated if we assume exponential decay of the SOL plasma density n_e and temperature T_e outside the last closed flux surface:

$$n_e(x) = n_e(0)\exp(-x/\lambda_n) \quad , \tag{21}$$

and

$$T_e(x) = T_e(0)\exp(-x/\lambda_T) \quad . \tag{22}$$

Here λ_n and λ_T represent the characteristic decay lengths of the density and temperature of the SOL plasma. We assume that the ion and electron temperatures are equal, $T_i \simeq T_e$, and take the particle flux to be

$$\Gamma_{\|} = n_e v_{\|} \sim n_e T_e^{1/2} \tag{23}$$

for particles with a velocity $v_{\|}$ along the field line and the heat flux to be

$$Q_{\|} = \gamma k T_e \Gamma_{\|} \sim n_e T_e^{3/2} \tag{24}$$

with γ the heat transfer coefficient. By using Eqs. (21) and (22) in Eqs. (23) and (24), we find the characteristic particle and heat flux decay lengths,

$$\lambda_\Gamma = \frac{2\lambda_n \lambda_T}{2\lambda_T + \lambda_n} \quad , \tag{25}$$

$$\lambda_q = \frac{2\lambda_n \lambda_T}{2\lambda_T + 3\lambda_n} \quad . \tag{26}$$

Experimental observations on TFTR[13] and JET[14,15] indicate that within the error bars of the measurements, $\lambda_T \simeq 2\lambda_n$. If we use this value in Eqs. (25) and (26), we get

$$\lambda_\Gamma \simeq \frac{4}{5}\lambda_n \quad , \tag{27}$$

$$\lambda_q \simeq \frac{4}{7}\lambda_n \quad . \tag{28}$$

The density scale length λ_n is often estimated by using Bohm diffusion. For the SOL plasma, as shown in Appendix B,

$$\lambda_n \simeq (D_{\mathrm{Bohm}}\tau_{\|})^{1/2} \quad , \tag{29}$$

where

$$D_{\mathrm{Bohm}} \sim kT_e/B \tag{30}$$

is the Bohm diffusion coefficient and

$$\tau_{\|} \sim L_c/v_{\|} \tag{31}$$

is the parallel flow loss time of the particles traveling along the magnetic field B, which have a typical connection length of $L_c \simeq q\pi R_0$ in the SOL before the particles hit the pump limiter.

The estimate of λ_n from Eq. (29) is reasonable when compared with the experimental observations.[15] Furthermore, Eq. (29) provides insight into the effects of the SOL parameters on the scale length and, in turn, the effects of design considerations on the pump limiter parameters.

III. MODULAR PUMP LIMITER SYSTEM

As noted in Section II, the power load in large tokamaks with $P_{\text{heating}} \geq 10$ MW will require multiple pump limiter modules. For our model calculations, we assume a system of N identical modules that can

1. remove particles at the necessary rate with an efficiency $\epsilon \geq \epsilon_{\text{crit}}$, where ϵ_{crit} is the critical efficiency for the device under consideration, and
2. remove a total power $P_{\text{T}} \geq 0.7 \times P_{\text{heating}}$.

In order to optimize particle exhaust, the limiter head surfaces must be designed to tolerate the highest heat fluxes possible. For the pump limiter model calculations, we require

1. the heat flux on the limiter surface $Q_{\text{n}} \leq Q_{\text{d}}$, where Q_{d} is the design value for the heat flux on the surface, and
2. the heat flux on the cooling channel at the leading edge $Q \leq Q_{\text{t}} > Q_{\text{d}}$, where Q_{t} is the design value for the heat flux on the leading edge.

Next we develop an expression for the system exhaust efficiency that combines some of these requirements (i.e., P_{T}, Q_{t}, and the diameter of the leading edge cooling channel) so that we can easily analyze the parameters that play an important role in the design of the individual modules and their realization from the viewpoint of engineering technology. We also discuss the location of the modules and shadowing considerations.

A. Pump Limiter System Particle Exhaust

In Section II, the exhaust efficiency of a modular pump limiter was given by Eq. (5). For the remaining discussions, we take the throat entrance width Δ to be the density scale length of the SOL, $\Delta \simeq \lambda_n$, and also assume $\lambda_T \simeq 2\lambda_n$. Then for a modular pump limiter

$$\epsilon_{\text{PL}} \simeq \frac{\epsilon_{\text{MC}}}{2} \exp(-x_{\text{h}}/\lambda_{\Gamma}) \ . \tag{32}$$

Here we have also used $\epsilon_R \simeq 0.7$.

At this point we make some assumptions about the power and particle sharing within the N modules in the system:

1. The total power is shared equally among the N modules,

$$P_{\text{T}} = N P_{\text{L}} \ ,$$

where P_{L} is the power received by a single limiter module.

2. Particle flux is not shared between modules within the same flux tube. That is, modules can "shadow" each other. This is a reasonable assumption, since the parallel particle flow $\Gamma_{\|}$ is much faster than the perpendicular diffusion, $\Gamma_{\perp}$. Therefore, on the time scale of parallel particle loss, $\tau_{\|}$, the flux tube may remain empty once the particles hit a limiter module. These assumptions reflect a conservative approach to the limiter design, since highly reliable performance of the modules in large tokamaks is strongly desired.

Let us now continue our discussion of particle exhaust with a pump limiter system. The system exhaust efficiency with N modules is

$$\epsilon = N\epsilon_{\mathrm{PL}} = \frac{N\epsilon_{\mathrm{MC}}}{2}\exp(-x_{\mathrm{h}}/\lambda_{\Gamma}) \ . \tag{33}$$

If $N\epsilon_{\mathrm{MC}} = 1$, then we achieve full flux coverage; that is, the efficiency is as high as possible:

$$\epsilon = \frac{1}{2}\exp(-x_{\mathrm{h}}/\lambda_{\Gamma}) \ . \tag{34}$$

The module coverage efficiency [Eq. (8)] therefore defines

$$N_{\mathrm{ff}} = \mathrm{Integer}\left(\frac{2\pi a}{qL_{\theta}}\right) \ , \tag{35}$$

where N_{ff} is the minimum number of modules that will provide full flux coverage in a given device. We have already established that the number of modules required to handle the power is $N = P_{\mathrm{T}}/P_{\mathrm{L}}$. Thus, we now need to consider the following possible cases:

1. $N > N_{\mathrm{ff}}$. This implies the presence of more than one module in the flux tube under consideration. Because we have assumed that the particle flux cannot be shared between modules in the same flux tube that shadow each other fully or partially, the second limiter cannot fully contribute to the particle removal. Only its unshadowed region within the flux tube, if there is one, can contribute. This is called "shadowing" and we therefore define a shadowing fraction,

$$f_{\mathrm{s}} = N_{\mathrm{ff}}/N < 1 \ , \tag{36}$$

and include it in Eq. (33),

$$\epsilon = f_{\mathrm{s}}N\epsilon_{\mathrm{PL}} = \frac{1}{2}\exp(-x_{\mathrm{h}}/\lambda_{\Gamma}) \ , \tag{37}$$

to obtain the "full flux coverage efficiency." In this case, it is clear that modules must be located so as to minimize shadowing.

2. $N < N_{\rm ff}$. In this case, $f_{\rm s} = 1$, but full flux coverage is not achieved. That is, $N\epsilon_{\rm MC} < 1$.
3. $N = N_{\rm ff}$. In this case, full flux coverage is achieved with no shadowing, $f_{\rm s} = 1$, and use of this set of modules is said to be optimum for achieving both power and particle removal.

Let us consider a pump limiter system with $N \geq N_{\rm ff}$. The system exhaust efficiency may be estimated by combining the total power [from Eqs. (B.7) and (B.8) in Appendix B],

$$P_{\rm T} = NP_{\rm L} = 2NL_\theta Q_0 \lambda_q (C_1 + C_2 N_{\rm ff}/N) \ ,$$

where $C_1 = \sqrt{2} - 1$, $C_1 + C_2 = 1$, and the heat flux at the tip of the leading edge,

$$Q_{\rm t} = Q_0 \exp[-(x_{\rm h} - x_{\rm t}/2)/\lambda_q] \ ,$$

with Eq. (34). We find

$$\epsilon \simeq 0.5 \left[\left(\frac{4N}{N_{\rm ff}} \right) \left(\frac{\pi a}{q} \right) \frac{\lambda_q Q_{\rm t} F_{\rm t}}{P_{\rm T}} (C_1 + C_2 N_{\rm ff}/N) \right]^{(\lambda_q/\lambda_{\rm r})} \ , \tag{38}$$

with $F_{\rm t} \equiv \exp(-x_{\rm t}/2\lambda_q)$, and we have also used the fact that $N_{\rm ff} L_\theta \simeq 2\pi a/q$. Here we should note that because we need full flux coverage in order to achieve the maximum possible system exhaust efficiency, we have $N \geq N_{\rm ff}$.

Equation (38) is very useful for estimating the exhaust efficiency of the overall modular pump limiter system, since for a given device, ϵ depends only on the parameters of the leading edge cooling channel (i.e., its diameter $x_{\rm t}$ and the design heat flux $Q_{\rm t}$). It is also clear that, for high exhaust efficiency in large tokamaks with extensive heating ($P_{\rm T} \simeq 10$ MW) and fueling ($\phi_{\rm ext} \simeq 50$ torr $\cdot$ L/s), small-diameter ($x_{\rm t} \simeq$ 1–2 cm) cooling channels are required to remove high heat loads ($Q_{\rm t} \simeq 3$ kW/cm^2). Therefore, the state of the art in engineering technology for high heat removal has a direct impact on the module design parameters for maximum efficiency.[11,12]

B. Location of Pump Limiter Modules and Shadowing Considerations

Modules should be located in the tokamak so as to attain the expected optimum performance. For particle removal, this means that modules must be located to minimize shadowing.

For the rest of the discussion, we assume a symmetric pump limiter system by considering an even number of modules N located in equal numbers at the top and at the bottom of the tokamak. Thus, the toroidal and poloidal separations between the modules are $\phi_s = 4\pi/N$ and $\theta_s = \pi$, respectively.

Figure 4 shows $N = 4$ modules, labeled A, B, C, and D. They are placed at the top and the bottom of the device with proper toroidal separation so that no shadowing occurs. For this case, we have the following relations for the dimensions shown in the figure:

$$\phi_s \geq 2\phi_{MC} = 2q\theta_{MC} \tag{39}$$

and

$$(q\theta_s + \phi_{MC}) \leq \phi_s^{T/B} \leq (q\theta_s - \phi_{MC}) \ , \tag{40}$$

where $\phi_s \equiv \phi_s^{T/T} = \phi_s^{B/B}$ is the toroidal separation angle between the modules at the top (or bottom) and $\phi_s^{T/B}$ (or $\phi_s^{B/T}$) is the toroidal separation angle between the top and the bottom modules. If $q\theta_s = \phi_s^{T/B}$, then all the modules shadow one another completely; otherwise, they partially shadow each other.

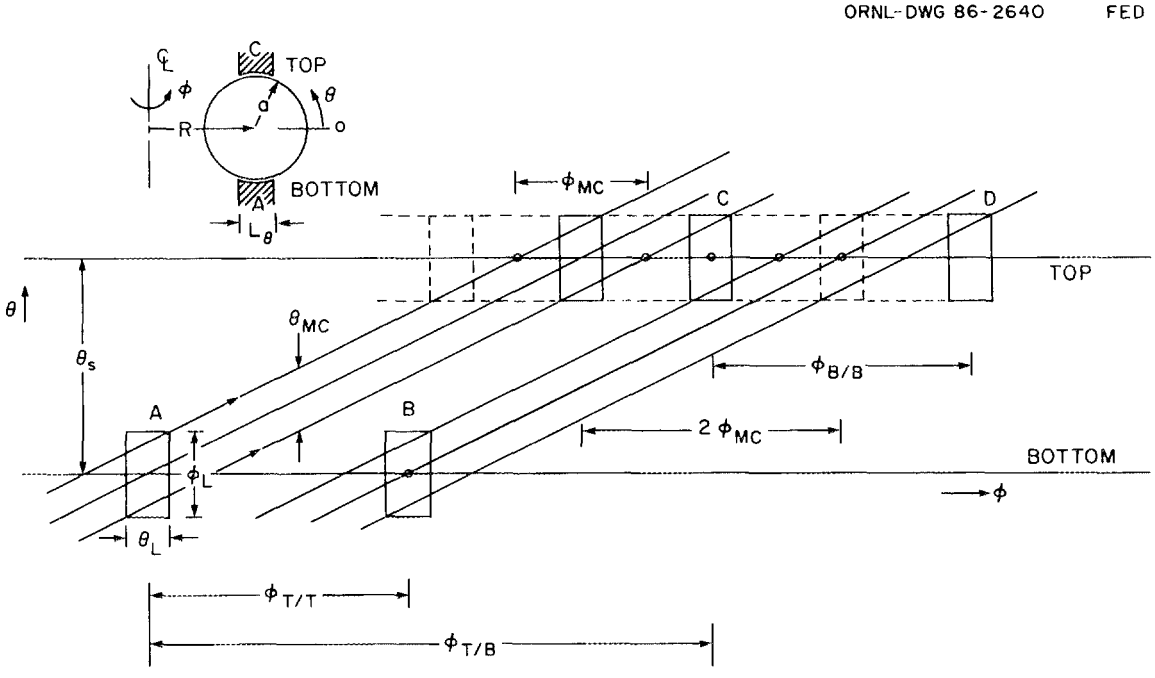

Fig. 4. Four modules located so that no shadowing between them occurs.

We rewrite Eq. (39) for our model case, in which $\phi_s - 4\pi/N$, as:

$$\frac{4\pi}{N} \geq 2q\theta_{\mathrm{MC}} \simeq 2q\theta_{\mathrm{L}} = 2q\frac{L_\theta}{a}$$

or

$$\frac{2\pi a}{q} \geq N L_\theta \ .$$

This gives $N\epsilon_{\mathrm{MC}} \leq 1$, which is simply the flux coverage relationship that we have discussed in Section III.A.

In order to understand the effects of partial shadowing between two modules on the system efficiency, we need to study such a case in more detail. To do that, we consider a system with only two modules, one at the top and the other at the bottom of the device with partial shadowing between them, as shown in Fig. 5. Then the system exhaust efficiency is written as

$$\epsilon = \epsilon_{\mathrm{R}} \times \sum_{j=1,2} \epsilon_{\mathrm{coll}}(j)\epsilon_{\mathrm{MC}}(j) \ , \tag{41}$$

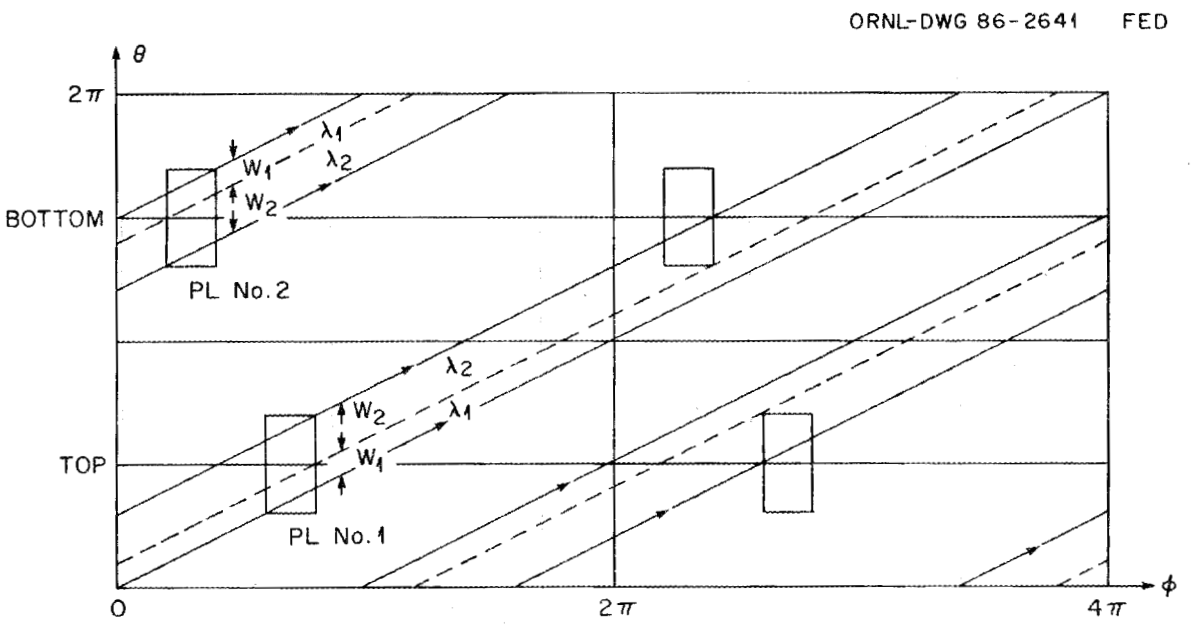

Fig. 5. Two modules located at $q = 2$ (the last closed surface). Slight shadowing occurs. The shadowed portion of the limiter is assumed to be idle for particle collection.

where

$$\epsilon_{\rm coll}(1) = \frac{w_1\lambda_1}{w_1\lambda_1 + w_2\lambda_2}\exp(-x_{\rm h}/\lambda_1)[1-\exp(-\Delta/\lambda_1)] + \frac{w_2\lambda_2}{w_1\lambda_1 + w_2\lambda_2}\exp(-x_{\rm h}/\lambda_2)[1-\exp(-\Delta/\lambda_2)]$$

with $L_\theta = w_1 + w_2$ and $\lambda_j \equiv \lambda_\Gamma(j)$. Similarly, $\epsilon_{\rm coll}(2) = \epsilon_{\rm coll}(1)$. Thus, we write

$$\begin{aligned}\epsilon_{\rm coll} &= \epsilon_{\rm coll}(1) = \epsilon_{\rm coll}(2) \\ &= \frac{\exp(-x_{\rm h}/\lambda_1)[1-\exp(-\Delta/\lambda_1)]}{1+(1-\alpha_{\rm s})/\alpha_{\rm s}\sqrt{2}} \\ &+ \frac{\exp(-\sqrt{2}x_{\rm h}/\lambda_1)[1-\exp(-\sqrt{2}\Delta/\lambda_1)]}{1+\alpha_{\rm s}\sqrt{2}/(1-\alpha_{\rm s})} \ . \end{aligned} \tag{42}$$

Here $w_1 = \alpha_{\rm s}L_\theta$, and (as we discuss in Appendix B) $\lambda_2 = \lambda_1/\sqrt{2}$, since there are two modules in the same flux tube that shadow each other.

The flux coverage fractions of the modules are

$$\epsilon_{\rm MC}(1) = q\frac{L_\theta}{2\pi a}$$

and

$$\epsilon_{\rm MC}(2) = q\frac{L_\theta - w_2}{2\pi a} = \alpha_{\rm s}\epsilon_{\rm MC}(1) \ .$$

Using this relation and Eq. (42) in Eq. (41), we find

$$\epsilon = (1+\alpha_{\rm s})\epsilon_{\rm MC}(1)\epsilon_{\rm R}\epsilon_{\rm coll}(1) \ . \tag{43}$$

For these calculations, we use typical values for the module head thickness, $x_{\rm t} \simeq \lambda_1$, and for the throat opening, $\Delta \simeq \lambda_1$. As a demonstration, if we take $\alpha_{\rm s} = w_1/L_\theta \simeq 0.5$ for the nonshadowed poloidal extent of the module, then from Eq. (42), we find $\epsilon_{\rm coll} \simeq 0.21$.

Now, for the case with no shadowing, on the other hand, the collection efficiency is

$$\epsilon_{\rm coll}({\rm NS}) = \exp(-x_{\rm h}/\lambda_1)[1-\exp(-\Delta/\lambda_1)] = e^{-1}(1-e^{-1}) \simeq 0.23 \ ,$$

which indicates that

$$\epsilon_{\rm coll}(1) = \epsilon_{\rm coll}(2) \simeq \epsilon_{\rm coll}({\rm NS}) \ .$$

Equation (43) then becomes

$$\epsilon \simeq (1+\alpha_{\rm s})\epsilon_{\rm MC}(1)\epsilon_{\rm R}\epsilon_{\rm coll}({\rm NS}) = \epsilon_{\rm MC}({\rm T})\epsilon_{\rm R}\epsilon_{\rm coll}({\rm NS})$$

or

$$\epsilon = 2 f_s \epsilon_R \epsilon_{MC} \epsilon_{coll} \qquad (N = 2) \ .$$

We find the shadowing fraction for this case to be $f_s = (1 + \alpha_s)/2$, and the total module coverage $\epsilon_{MC}(T) = \epsilon_{MC}(NS)(1 + \alpha_s)$, where $\epsilon_{MC}(NS) = \epsilon_{MC}(1)$ is the nonshadowed module coverage.

In Fig. 6, we display the normalized collection efficiency, $\epsilon_{coll}(N_s, \alpha_s)/\epsilon_{coll}(NS)$ for $N_s = 2$ and for $N_s = 3$ modules partially sharing the same flux tube for various values of α_s, from full shadowing ($\alpha_s = 0$) to no shadowing ($\alpha_s = 1$). For $N_s = 2$ we observe that, if $\alpha_s \geq 0.3$, the error in estimating $\epsilon_{coll}(\alpha_s)$ from $\epsilon_{coll}(NS)$ is $\leq 10\%$. On the other hand, for $N_s = 3$, the error is $\leq 1\%$. This exercise suggests that it may be possible to use $\epsilon_{coll}(NS)$ in the efficiency calculations without introducing large errors. Therefore, for the remaining discussion, we assume that $\epsilon_{coll}(N_s, \alpha_s) \simeq \epsilon_{coll}(NS)$ as given by Eq. (10). We may now generalize the case for an even number of modules N ($\geq N_{ff}$). The composite exhaust efficiency may be written as

$$\epsilon = \epsilon_R \epsilon_{coll}(NS) \sum_{j=1,N} \epsilon_{MC}(j) \ ,$$

where

$$\sum_j \epsilon_{MC}(j) = \epsilon_{MC}(NS) N (1 + \alpha_s)/2 \ , \tag{44}$$

with α_s the nonshadowed poloidal extent of the module and $\epsilon_{coll}(NS)$ and $\epsilon_{MC}(NS)$ the collection and the module coverage efficiencies, respectively, as if no shadowing were present.

We may use the expression for the composite exhaust efficiency to obtain the shadowing fraction f_s by writing

$$\epsilon = f_s N \epsilon_R \epsilon_{coll}(NS) \epsilon_{MC}(NS) \ , \tag{45}$$

from which we find

$$f_s = N_{ff}/N = (1 + \alpha_s)/2 \ , \tag{46}$$

and the fraction of the nonshadowed module poloidal extent becomes

$$\alpha_s = 2(N_{ff}/N) - 1 \ . \tag{47}$$

For example, if there is no shadowing ($N = N_{ff}$), then $\alpha_s = 1$ and the shadowing fraction becomes $f_s = 1$.

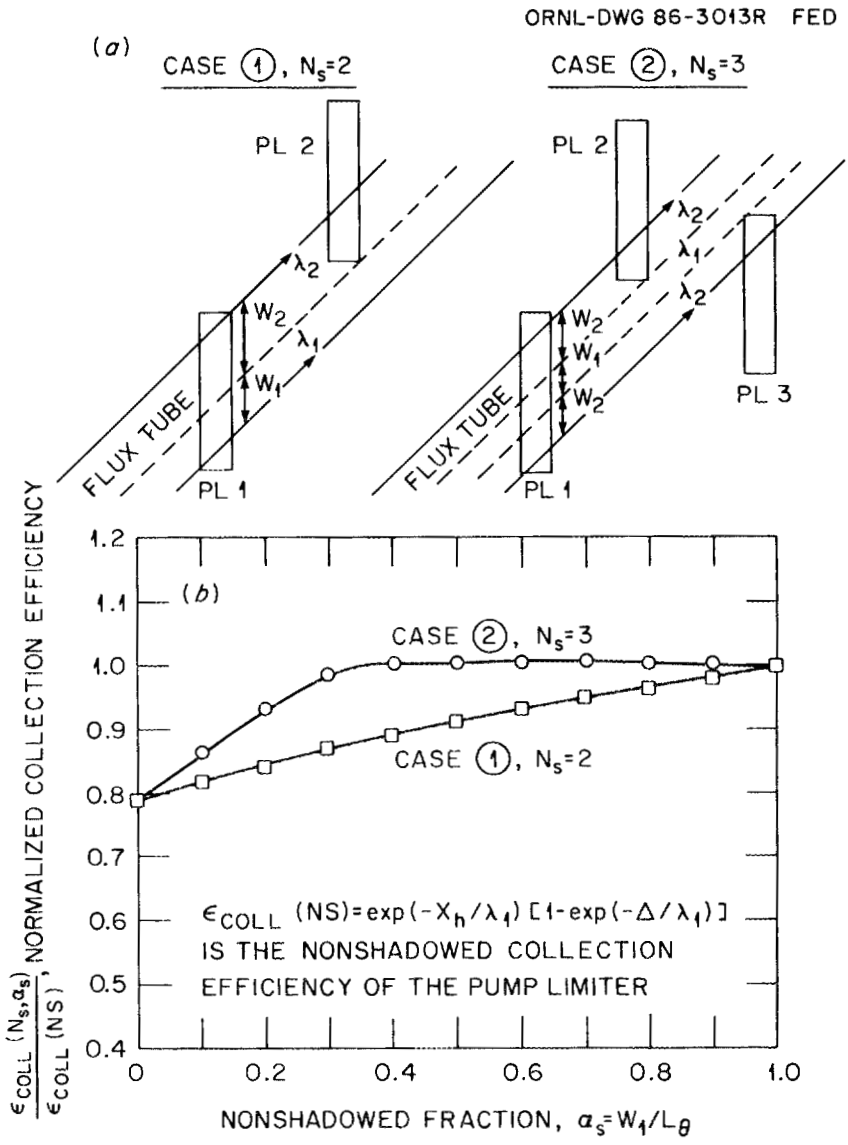

Fig. 6. (a) Typical shadowing cases: $N_s = 2$ and $N_s = 3$ modules, partially shadowing each other. (b) Normalized collection efficiency $\epsilon_{\rm coll}(N_s, \alpha_s)/\epsilon_{\rm coll}({\rm NS})$ for various values of the nonshadowed fraction α_s from full shadowing ($\alpha_s = 0$) to no shadowing ($\alpha_s = 1$).

The explicit forms of the terms in Eq. (45), $\epsilon_{\rm R}\epsilon_{\rm coll}({\rm NS})$ and $\epsilon_{\rm MC}({\rm NS})$, given here for completeness, are

$$\epsilon_{\rm R}\epsilon_{\rm coll}({\rm NS}) = \frac{1}{2}\exp(-x_{\rm h}/\lambda_{\rm r}) \tag{48}$$

and

$$\epsilon_{\rm MC}({\rm NS}) \simeq qL_\theta/2\pi a\ . \tag{49}$$

IV. TORE SUPRA PUMP LIMITER SYSTEM

The Tore Supra[1] tokamak, which is about the same size as TFTR, has a major radius $R_0 \simeq 2.4$ m, a minor radius $a \simeq 0.7$–0.85 m, a toroidal magnetic field $B \simeq 4.5$ T (produced by superconducting magnets with a maximum field of 9 T at 4.2 K), and a maximum plasma current $I_p \simeq 1.7$ MA. The typical discharge duration is expected to be 30 s; auxiliary heating consists of 7 MW of NBI and a total of about 16 MW of ion cyclotron heating (ICH) and lower hybrid heating (LHH). It is expected that during full-scale operation of the device, up to $\simeq$15 MW of heating power will be delivered by two of the three heating techniques. Tore Supra will also use pellet injection ($\phi_p \simeq 40$ torr $\cdot$ L/s) for core plasma fueling to permit operation at high density ($\sim 10^{20}$ m^{-3}).

The large external sources ($\phi_{ext} \simeq 50$ torr $\cdot$ L/s) resulting from NBI and pellet fueling must be accommodated. Design calculations with the model described in this paper indicate that up to seven pump limiter modules will be needed to handle the particle exhaust to prevent exposure of the limiter surfaces and their leading edges to higher heat fluxes than can be tolerated with active cooling ($Q_t \lesssim 3$ kW/cm^2).

The required system exhaust efficiency for density control with external fueling in Tore Supra can be estimated using Eq. (3). In Tore Supra, the expected plasma efflux $N_e/\bar{\tau}_p \simeq 2 \times 10^{22}$ s^{-1} for a global particle confinement time of $\bar{\tau}_p \simeq 0.1$ s, and the planned total external fueling $\phi_{ext} \simeq 40$–50 torr$\cdot$L/s that must be exhausted by the pump limiters to maintain particle balance. Thus, the overall required exhaust efficiency of the pump limiter system is $\epsilon \simeq 10$–15%.

We can now estimate the design parameters for the pump limiter system. If the device is operated with $I_p = 1.7$ MA and a plasma radius of $a \simeq 0.75$ m, then $q(a) \simeq 3$ and the estimated SOL density scale length[1] is $\lambda_n \simeq 3$ cm (as calculated in Appendix B), which gives $\lambda_\Gamma \simeq 2.4$ cm and $\lambda_q \simeq 1.7$ cm for $\lambda_T \simeq 2\lambda_n$ [Eqs. (27) and (28)]. We assume that about 60% of a moderate heating power of $P_{heating} \simeq 10$ MW ends up on the limiters, so $P_T \simeq 6$ MW must be removed by the modules. Using these parameters in the exhaust efficiency expression, Eq. (38), we get $\epsilon = f(Q_t, x_t)$; that is, ϵ depends only on the diameter x_t and the design heat flux Q_t of the cooling channel at the module's leading edge. In Fig. 7, we have plotted ϵ for values of $x_t = 1$–2 cm and $Q_t = 1$–3 kW/cm^2 for two cases: (1) $N/N_{ff} = 1$ and (2) $N/N_{ff} = 1.5$. The figure also shows the limiter head thickness x_h, since for the full flux coverage pump limiter system we have $x_h = -\lambda_\Gamma \ln 2\epsilon$ from

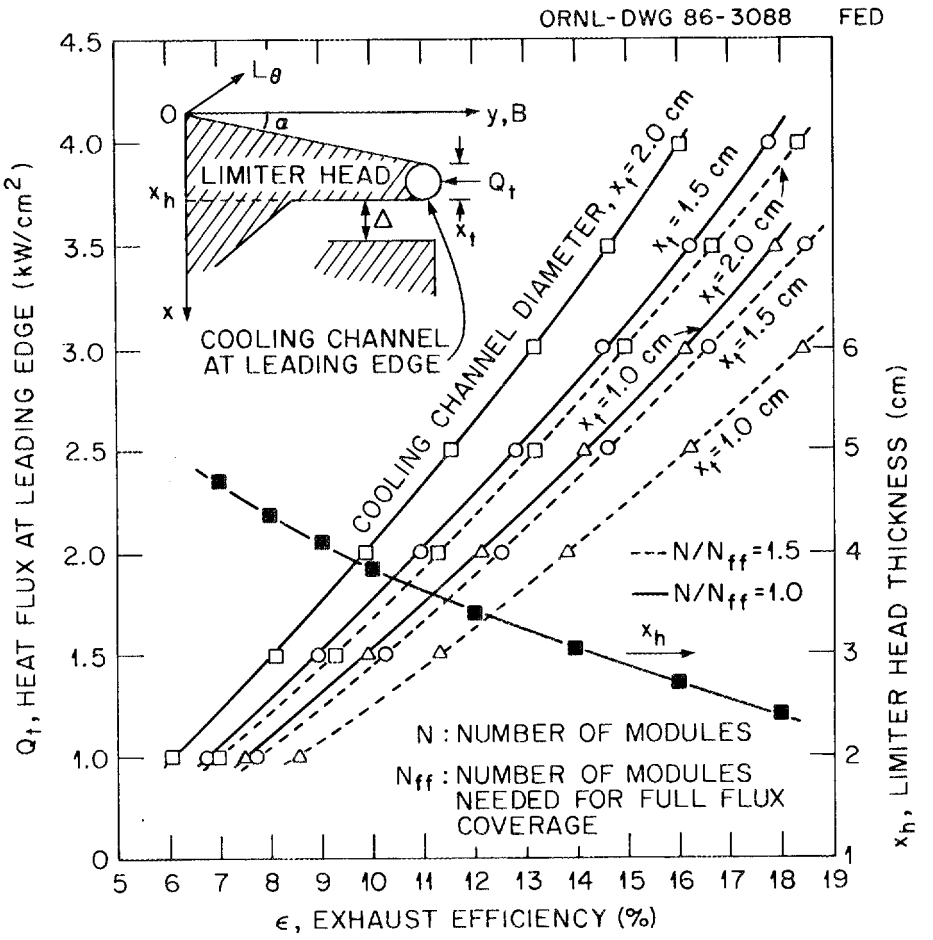

Fig. 7. The leading edge heat flux Q_t versus the system exhaust efficiency ϵ for various values of the x_t for the Tore Supra pump limiter system. The module head thickness x_h is also shown.

Eq. (34). Furthermore, the poloidal extent L_θ must satisfy the requirement for full flux coverage, $N_{ff} L_\theta \simeq 2\pi a/q$.

As we see from Fig. 7, in order to meet the required system exhaust efficiency $\epsilon \simeq 15\%$ and $Q_t \leq 3$ kW/cm^2, the cooling channel diameter should be $x_t \simeq 2$ cm, and the number of modules needed is $N \simeq 1.5 N_{ff}$. The module head thickness then becomes $x_h \simeq 2.9$ cm in order to have $\epsilon \simeq 15\%$. These values for the leading edge parameters are within the reach of existing heat removal technology.[11,12]

The toroidal extent L_ϕ of the limiter head can be estimated by requiring the heat flux on the surface (where $x = 0$) to be less than or equal to the design value of Q_d,

$$Q_{\rm n}(x=0) = 2(x_{\rm h} - x_{\rm t})\frac{Q_{\parallel}(x=0)}{L_\phi} \leq Q_{\rm d} \ ,$$

where

$$Q_{\parallel}(x=0) = Q_0 = Q_{\rm t}\exp[(x_{\rm h} - x_{\rm t}/2)/\lambda_q] \ . \tag{50}$$

Using the values we have assumed for $Q_{\rm t}$, $x_{\rm h}$, and $x_{\rm t}$, and taking $Q_{\rm d} \simeq$ 300–500 W/cm, we find

$$L_\phi = 2(x_{\rm h} - x_{\rm t})\frac{Q_0}{Q_{\rm d}} = 38\text{–}40 \text{ cm} \ .$$

Because the vertical ports on Tore Supra are small, $L_\phi \simeq 40$ cm has been chosen. For this case, the angle of the limiter surface to the magnetic field will be $\alpha \simeq 2.2°$.

The poloidal extent L_θ of the module head and the number of modules in the system can be estimated from the total power received by the limiter system and from the constraint placed on L_θ by the device port dimensions. From the power handling requirement, ignoring the effects of shadowing, we find

$$NL_\theta \simeq \frac{P_{\rm T}}{2Q_0\lambda_q} \simeq 200 \text{ cm} \ .$$

Here, we have used $P_{\rm T} = 6$ MW and $Q_0 \simeq 9$ kW/cm^2, which was calculated from Eq. (50) with $Q_{\rm t} \simeq 3$ kW/cm^2. On the other hand, for the system with full flux coverage we need $N_{\rm ff}L_\theta \simeq 150$ cm. Thus, by combining these two requirements, we find $N/N_{\rm ff} \simeq 1.5$, and this value has been used in Fig. 7 to estimate the system efficiency. For device operation at higher heating power (15 MW) in the future, it is desirable to have $NL_\theta > 200$ cm. Because L_θ is limited by the port size to 40 cm, the ability to handle additional power depends on the number of modules N. For 15 MW of heating power, $N = 6$–7 is needed.[12]

For this study, since we assume a symmetric modular configuration in the device, we take $N = 6$ modules. This satisfies the requirement of $N = 1.5N_{\rm ff}$, where the minimum number of modules needed for full flux coverage is $N_{\rm ff} \simeq 4$ for $L_\theta = 40$ cm, the port size of Tore Supra. The modules are placed at the top and the bottom of the device in equal numbers, $N/2$, separated toroidally by $\phi_{\rm s} = 4\pi/N = 120°$, as shown in Fig. 8. A perspective view of the planned vertical pump limiter module[16] of Tore Supra is shown in Fig. 9. The module head is made of copper tubes protected with graphite brazed armor. The titanium getters in the pumping chamber can provide the pumping speed of 25,000 L/s.

Because $N\epsilon_{\rm MC} \simeq 1.5 > 1$, these modules shadow each other as shown in Fig. 8. We can estimate the shadowing fraction $f_{\rm s}$, from its definition in Eq. (36), to be

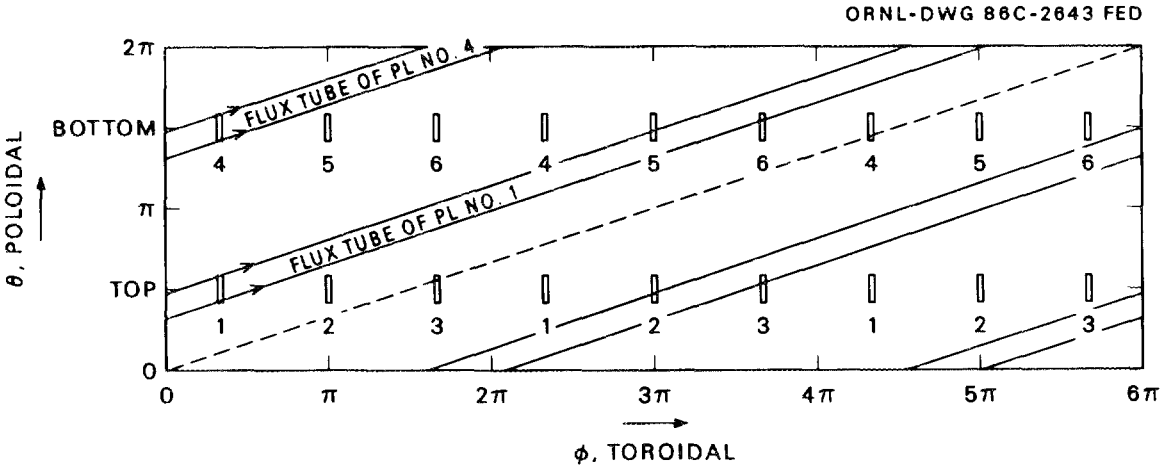

Fig. 8. Locations of $N = 6$ modules for Tore Supra. Modules are placed at the top and bottom of the device and $\phi_s = 120°$ apart toroidally. There is some shadowing between modules 1 and 6, 2 and 4, and 3 and 5.

$f_s = 0.65$. The total system exhaust efficiency is then estimated from Eq. (45) using the parameters obtained earlier for the module, $x_t = 2.9$ cm for the head thickness and $L_\theta = 40$ cm for the poloidal extent. Using Eqs. (48) and (49), we find the nonshadowed module efficiency to be $\epsilon_{PL}(NS) \simeq 4\%$ and, for $N = 6$ modules, $Nf_s \simeq 3.9$; then, from Eq. (45), the total system efficiency $\epsilon \simeq 15\%$. This is the same value, of course, that we have obtained from Fig. 7 using $x_t \simeq 2$ cm and $Q_t \simeq 3$ kW/cm^2. We can also estimate the nonshadowed poloidal extent of the module from Eq. (47), and we find $\alpha_s \simeq 0.33$, as seen in Fig. 8.

The power sharing within the various parts of the module can be estimated by using Eqs. (14)–(17). For this case, we find $P_s/P_L \simeq 40\%$ on the module surface, $P_t/P_L \simeq 44\%$ at the leading edges, and $P_n/P_L \simeq 16\%$ on the neutralizer plate. The total power removed by this module is $P_L = P_T/N = 1$ MW.

Here we should note that we have not used a model for the limiter blade that was shaped for uniform heat load.[8] The module head thickness in the constant heat flux model was given by[8] $x_h = \lambda_q \ln(Q_0/Q_d)$, and if we use our values of $Q_0 \simeq 9$ kW/cm^2 and $Q_d \simeq 0.5$ kW/cm^2 for the surface that includes the leading edge, we have $x_h \simeq 5$ cm. That reduces the exhaust efficiency to $\epsilon \simeq \frac{1}{2}\exp(-x_h/\lambda_\Gamma) \simeq 6\%$.

ORNL--DWG 86-2171 FED

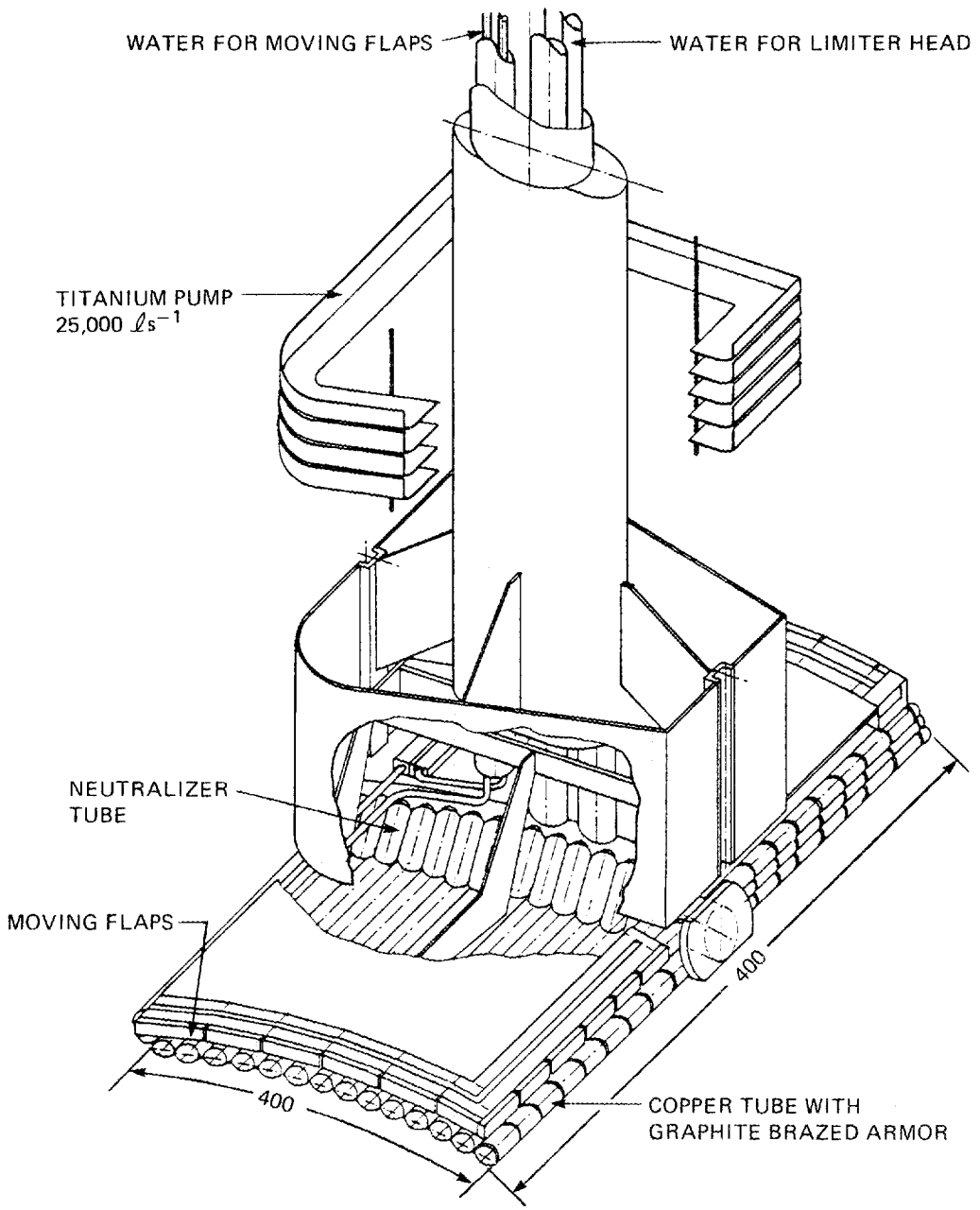

Fig. 9. Perspective view of the planned vertical pump limiter module of Tore Supra (Ref. 16). The module head is 40 cm × 40 cm and is made of copper tubes with graphite brazed armor protection. The titanium getters in the pumping chamber can provide a pumping speed of 25,000 L/s. The limiter is designed to handle 1 MW of power removal. The head thickness is expected to be $x_h \simeq 2.5$–3 cm.

V. EFFECTS OF MAGNETIC FIELD RIPPLE ON THE LIMITER MODULE

The finite number of toroidal field coils in tokamaks inevitably gives rise to a magnetic field ripple $\delta = (B_{\max} - B_{\min})/(B_{\max} + B_{\min})$, where $B_{\max}$ and $B_{\min}$ are the magnitudes of the field at the coil and at the coil midplane, respectively. This ripple will affect our model calculations for the pump limiter module, since we assume an ideal toroidal magnetic field. For example, as we discuss later, the radial component of the field B_r that results from this ripple introduces a so-called ripple angle $\theta_\delta = \tan^{-1}(B_r/B_{\text{toroidal}})$ in the particle flow and may lead to an increase in the modeled heat flux at the face of the pump limiter, as well as a displacement of the module leading edge further into the SOL.

It can be shown that the ripple angle θ_δ is zero on the coil and coil midplane, but it reaches its maximum at a toroidal angle of $\psi = \pi/2N_{\text{coil}}$, where $\psi = 0$ is the coil plane, as shown in Fig. 10, and N_{coil} is the number of toroidal field coils. We may model the variation of the toroidal field within the coils to be[17] $B_\psi \sim (1 - \delta \cos N_{\text{coil}}\, \psi)$ and use $\nabla \cdot \mathbf{B} = 0$ to calculate the radial field component B_r. Then the maximum value of the ripple angle is given by[18]

$$\tan \theta_\delta \simeq 0.25 \delta N_{\text{coil}} (a/R_0) \ . \tag{51}$$

Here we have also assumed that the radial profile of the ripple can be modeled as $\delta(r) \sim (r/a)^4$. This form for the radial dependence of the ripple is also observed from the magnetic field calculations of the Tore Supra coil configuration.[19]

The resulting field from the ripple B_r will cause a radial displacement of the magnetic field line, which may be estimated from the field line equation:

$$\delta r = \int_0^\psi d\psi \ R(B_r/B_\psi) \ .$$

As shown in Fig. 10, the value of this δr displacement when the ripple angle becomes maximum (where $\psi = \pi/2N_{\text{coil}}$) is given by[18]

$$\delta r(\max) \equiv \delta r_{\max} \simeq \delta(r) a/6 \ . \tag{52}$$

In order to further study the effects of ripple on the pump limiter, we may assume, for simplicity, that the SOL boundary is displayed about δr from the module surface, as shown in Fig. 11. The field ripple simply allows the particles to flow in

ORNL-DWG 86-2991 FED

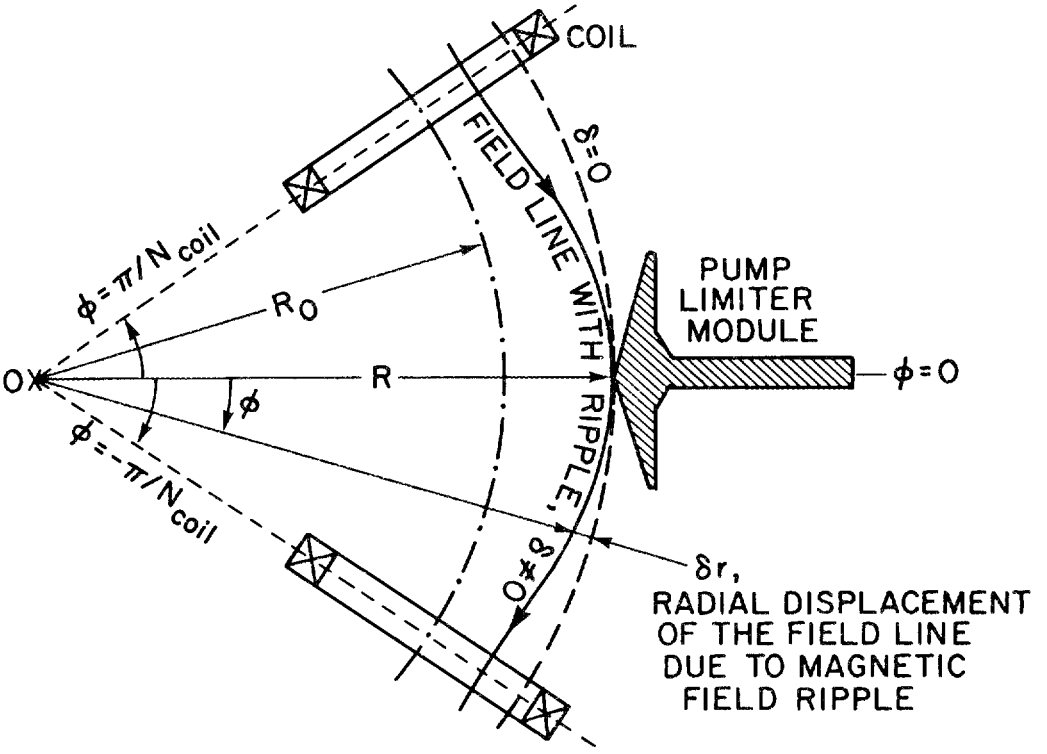

Fig. 10. Radial displacement δr of the field line as a result of magnetic field line ripple and its effect on the pump limiter module.

ORNL-DWG 86-3089 FED

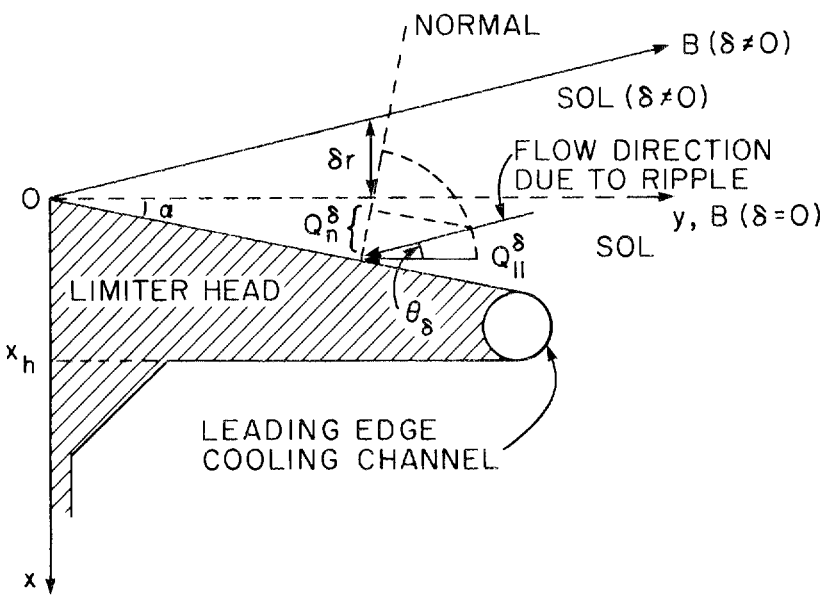

Fig. 11. Effects of field ripple on the module. The flow direction changes, and the leading edge is positioned further into the SOL.

a direction closer to the normal of the limiter surface than that for which it was modeled. We now compare the heat fluxes with and without ripple.

Due to the radial displacement, we have for the SOL heat flux

$$Q_{\parallel}^{\delta} = Q_0 \exp[-(x + \delta r)/\lambda_q] \ , \tag{53}$$

and the resulting module surface heat flux is

$$Q_n^{\delta} = Q_{\parallel}^{\delta} \sin(\alpha + \theta_\delta) \ . \tag{54}$$

Now, by comparing Eq. (54) to the case with no ripple, $Q_n = Q_0 \exp(-x/\lambda_q) \sin\alpha$, we find

$$Q_n^{\delta}/Q_n = \exp(-\delta r/\lambda_q) \sin(\alpha + \theta_\delta)/\sin\alpha \ . \tag{55}$$

Similarly, the SOL particle flux is given by

$$\Gamma_{\parallel}^{\delta} = \Gamma_0 \exp[-(x + \delta r)/\lambda_\Gamma] \ ,$$

which implies that the particle collection of the module is affected by δr displacement. Therefore, the collection efficiency of the pump limiter with ripple $\epsilon_{\rm coll}^{\delta}$ is reduced, and

$$\epsilon_{\rm coll}^{\delta}/\epsilon_{\rm coll} = \exp(-\delta r/\lambda_\Gamma) \ . \tag{56}$$

We should also note that since the field lines come to the neutralizer plate of the module with an angle due to the ripple, the particle removal efficiency $\epsilon_{\rm R}$ is also expected to be somewhat reduced.

One alternative to minimize the effect of ripple on particle collection is to shape the module surface to the local magnetic field line.

For the Tore Supra tokamak, $N_{\rm coil} = 18$, $R_0/a \simeq 3$, and the magnetic field ripple[19] is $\delta \simeq 2.7\%$ at the vertical pump limiter location, $a \simeq 0.75$ m. We find the ripple angle, from Eq. (51), to be $\theta_\delta \simeq 2.3°$, and this occurs where $\psi \simeq 5°$ or $y \simeq 21$ cm, that is, at the leading edge of the module, since its toroidal extent is $L_\phi = 40$ cm. The surface angle α of the circular cooling channel at the leading edge is much larger than θ_δ as shown in Fig. 12(b), and using the radial field displacement estimated from Eq. (52), $\delta r_{\rm max} \simeq 0.34$ cm in Eq. (55), we find $Q_n^{\delta}/Q_n \simeq 0.82$. Similarly, $\epsilon_{\rm coll}^{\delta}/\epsilon_{\rm coll} \simeq 0.87$. These estimates indicate that the field ripple in Tore Supra will not greatly affect the results for the vertical modules that we have discussed earlier.

ORNL-DWG 86-3124 FED

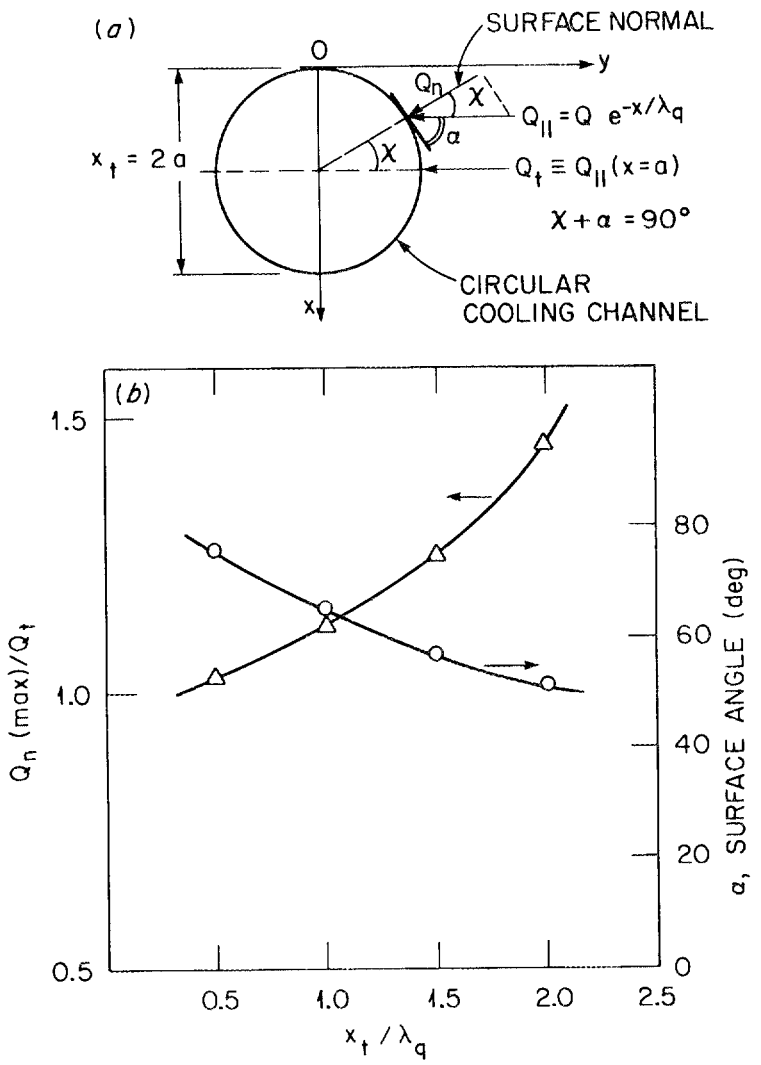

Fig. 12. The maximum value of the surface heat flux $Q_n(\max)$ and the surface angle α for a circular cooling channel as a function of x_t/λ_q where x_t is the diameter of the cooling channel.

VI. DISCUSSIONS

In this work, we have investigated a pump limiter system that consists of a number of modules for large tokamaks. We have developed a model for estimating the system exhaust efficiency in terms of the parameters of an actively cooled module leading edge and the power load that must be removed. The choice of locations for the modules was also discussed, and the effects of shadowing between modules on particle and power removal were examined. The results were then applied to Tore Supra and the conceptual design parameters of the limiter system were estimated.

In our model calculations, we have assumed a cylindrical geometry, and, for the sake of simplicity, the toroidal effects were ignored. A more realistic approach to the geometry has been left for future study.

We have ignored ionization of the particles in the SOL. This process may affect the profiles and lead to flux amplification[20] for ions hitting the limiter; this may eventually alter the exhaust efficiency of the system.

We have also neglected a number of relevant issues in this study:

1. The finite poloidal beta β_p of the core plasma causes a Shafranov shift, which may in turn affect the SOL plasma by producing a slight elongation. If this effect becomes significant, then the top and bottom limiters have longer characteristic scale lengths and could be more efficient for particle removal.
2. Variations in the plasma current may affect the scale lengths and also the flux coverage shadowing between the modules. The edge safety factor $q(a)$ should be selected so as to ensure optimum pump limiter operation.
3. Highly asymmetrical particle flow, as observed on almost all tokamaks, from the ion-drift direction may enhance the particle collection, if particles are collected from the ion side only. A collector slot on the electron-drift side would represent a loss term only if the two sides were connected within the pump limiter chamber. A movable flap on the electron side is a possible solution.
4. Disruptions of the plasma current and runaway electrons must be considered in the design of the limiter surface. For example, the limiter eddy currents should be kept as low as possible during disruptions. Also, the amount of thermal energy deposited on the limiter surface can be as much as 4 MJ/m^2 within 10 ms or less during a plasma disruption. This may lead to ablation layer thickness in the micrometer range. This effect can be very deleterious to the protective cladding of the cooling channel or to the limiter surface. Therefore, more detailed analysis must be incorporated in the design of the limiter. Work

is under way in this area for the present design of the Tore Supra pump limiter system. Runaway electrons have very short scale lengths ($\lambda_q < 1$ cm) in the SOL. Therefore, their energy is very concentrated when deposited on the limiter. The cooling lines of the limiter must be protected against this localized heat deposition by a runaway electron beam.[12]

As the long-pulse operation of tokamaks with high auxiliary heating power becomes a reality, use of some technique for particle and power removal is inevitable. In this work, we have discussed a modular pump limiter system as one solution of this problem. In this regard, we are hopeful that engineering technology for the high heat removal will soon achieve the routine application phase that we would like to have on the limiters.

Experiments scheduled to begin in late 1987 on the Tore Supra tokamak will provide the needed database for the performance of the modular pump limiter system. At the same time, alternatives with more efficient particle removal (>10%) techniques should be explored.

ACKNOWLEDGMENTS

The authors gratefully acknowledge valuable discussions with P. Deschamps. The continuous support and encouragement of R. Aymar and L. A. Berry are also appreciated.

REFERENCES

1. P. DESCHAMPS et al., "Power Exhaust and Plasma-Surface Interaction Control in Tore Supra," *J. Nucl. Mater.*, **128 & 129**, 38 (1984).
2. P. K. MIODUSZEWSKI et al., "Particle Removal with Pump Limiters in ISX-B," *J. Nucl. Mater.*, **121**, 285 (1984).
3. R. BUDNY et al., "Initial Results from the Scoop Limiter Experiment in PDX," *J. Nucl. Mater.*, **121**, 294 (1984).
4. R. W. CONN et al., "Advanced Limiter Test (ALT-I) in the TEXTOR Tokamak—Concept and Experimental Design," in *Proc. 10th Symposium on Fusion Technology (SOFT)*, Vol. 1, p. 497, Pergamon Press, Elmsford, N.Y. (1983).
5. S. A. COHEN et al., "The PLT Rotating Pumped Limiter," *J. Nucl. Mater.*, **128 & 129**, 430 (1984).
6. R. W. CONN et al., "An Advanced Pump Limiter Experiment of Large Toroidal Extent—ALT II," *J. Nucl. Mater.*, **121**, 350 (1984).
7. R. W. CONN et al., "Tokamak Pump Limiters," *J. Nucl. Mater.*, **128 & 129**, 407 (1984).
8. P. K. MIODUSZEWSKI, "Advanced Limiters," in *Physics of Plasma-Wall Interactions in Controlled Fusion*, Eds. D. E. POST, R. BEHRISCH, p. 891, Plenum Publishing Corp., New York (1986).
9. K. H. DIPPEL et al., "ALT-I Pump Limiter Results on TEXTOR," in *Proc. 10th Int. Conf. Plasma Physics and Controlled Fusion Research*, London, 1984, Vol. I, p. 249, International Atomic Energy Agency, Vienna (1985).
10. A. E. PONTAU et al., "Initial ALT-I Pump Limiter Studies on TEXTOR," *J. Nucl. Mater.*, **128 & 129**, 434 (1984).
11. S. L. MILORA, S. K. COMBS, and C. A. FOSTER, "A Numerical Model for Swirl Flow Cooling in High-Heat-Flux Particle Beam Targets and the Design of a Swirl-Flow-Based Plasma Limiter," *Nucl. Eng. Des./Fusion*, **3**, 301 (1986).
12. J. B. WHITLEY et al., "Engineering Considerations for the Tore Supra Pump Limiter," in *Proc. 14th Symposium on Fusion Technology (SOFT)*, in press, 1986.
13. D. M. MANOS et al., "Edge Probe Results During Gettered and Ungettered TFTR Discharges," *Bull. Am. Phys. Soc.*, **30**, 1523 (1985).

14. S. K. ERENTS et al., "Parameters of the JET Edge Plasma During OH, RF and Open Boundary Experiments from Langmuir/Heat Flux Probes," *Bull. Am. Phys. Soc.*. **30**, 1525 (1985).
15. P. C. STANGEBY, "Edge Probes," *J. Nucl. Mater.*, **145 & 146**, 105 (1987).
16. R. AYMAR, B. BERTRAND, et al., "Implementation of the Plasma Wall Interaction Control Systems in Tore Supra," TS-51-85-04, Association Euratom-CEA, Cadarache, France (December 1985).
17. N. A. UCKAN et al., "Toroidal Field Ripple Effects in Large Tokamaks," in *Proc. Sixth Symposium on Engineering Problems of Fusion Research*, p. 1105, Institute of Electrical and Electronics Engineers, New York (1975).
18. C. C. KLEPPER, T. UCKAN, P. K. MIODUSZEWSKI, R. T. McGRATH, and P. HERTOUT, "Consideration of the Magnetic Field Ripple in the Design of Plasma Edge Components," ORNL/TM-10428, Oak Ridge National Laboratory, Oak Ridge, Tennessee (1987).
19. P. HERTOUT, CEA, Cadarache, France, private communication, 1986.
20. R. BUDNY et al., "Edge Probe Studies of TFTR Plasmas at High Neutral Beam Injection Power," *Bull. Am. Phys. Soc.*, **31**, 1448 (1986).
21. P. C. STANGEBY, "The Plasma Sheath," in *Physics of Plasma-Wall Interactions in Controlled Fusion*, Eds. D. E. POST, R. BEHRISCH, p. 41, Plenum Publishing Corp., New York (1986).

Appendix A: Calculation of $Q_n(\max)$ for a Circular Cooling Channel

We need to calculate the maximum value of the heat flux and its location for a circular cooling channel, which is used in our model for the leading edge of the pump limiter modules.

From Fig. 12(a), we write

$$Q_n = Q_0(y/a)\exp(-x/\lambda_q) \quad ,$$

where $y^2 = a^2 - (x-a)^2$ is the equation for a circle. By defining $G(x) \equiv aQ_n/Q_0$ and searching for the value of $x = x_m$ that makes $G(x)$ maximum, we find

$$x_m/\lambda_q = 0.5[1 + (x_t/\lambda_q) - \sqrt{1 + (x_t/\lambda_q)^2}] \ ,$$

where $x_t = 2a$ is the diameter of the cooling channel. The surface angle α is also calculated from $\cos\alpha = (1 - x_m/a)$ and $\chi = 90° - \alpha$ is the angle between the heat flow $Q_{||}$ and the surface normal.

In Fig. 12(b), we display the values of $Q_n(x_m)/Q_t$ and α for various values of x_t/λ_q, where $Q_t = Q_0\exp(-x_t/2\lambda_q)$. For example, for $x_t/\lambda_q \simeq 1$, we have $Q_n(x_m)/Q_t \simeq 1$, $\alpha \simeq 65°$, $\chi \simeq 25°$, and $x_m/\lambda_q \simeq 0.29$.

Appendix B: Parameters of SOL Plasma

In order to carry out the calculations for the pump limiter system for a given device, we need to know the characteristics of the SOL plasma—for instance, its density and temperature as well as their scale lengths. In this Appendix, we discuss estimating these parameters in terms of given device characteristics, such as P_T, $N_e/\bar{\tau}_p$, $q(a)$, a, and R_0.

The characteristic density scale length λ_n of the SOL plasma, whose boundary is defined by the limiter, $x = 0$, can be estimated by assuming a one-dimensional model of the SOL parameters if $\lambda_n \ll a$. From the particle balance relation, we have

$$D_\perp \frac{d^2 n_e}{dx^2} = \frac{n_e}{\tau_{||}} \quad , \tag{B.1}$$

where $D_\perp$ is the particle diffusion coefficient that can be taken to be in the form given by Bohm, $D_\perp \sim T_e/B$, and $\tau_{||} = L_c/v_{||}$ represents the parallel flow loss time of the particle along the field line in the SOL.

The solution of Eq. (B.1) is found by substituting $n_e \sim \exp(-x/\lambda_n)$; then

$$\lambda_n = (D_\perp \tau_\parallel)^{\frac{1}{2}} \quad . \tag{B.2}$$

For an axisymmetric toroidal device the connection length $L_c = L_\parallel/2 = q\pi R_0$ and the flow velocity[7] $v_\parallel \simeq 0.3c_s$, where

$$c_s = \left[\left(\frac{5}{3}T_i + T_e\right)\Big/ m_i\right]^{0.5}$$

is the ion sound speed and $T_i \simeq T_e$ is assumed for the calculations. If N_s limiters are sharing the same flux tube, then $L_c \simeq q\pi R_0/N_s$ and, in turn, $\lambda_{neff} = \lambda_n/\sqrt{N_s}$. For example, if $N_s = 2$, then the effective density scale length becomes shorter, about 70% of that for one limiter. Therefore, if shadowing occurs between the modules, the collection efficiency may drop because $\epsilon_{coll} \sim \exp(-x_h/\lambda_{eff})$.

In order to calculate the density scale length, we need to estimate the electron temperature T_e at the SOL, with the total particle outflux $N_e/\bar{\tau}_p$ and the available power P_T known. From the particle and power balance equations at the plasma boundary, $x = 0$,

$$N_e/\bar{\tau}_p = \Gamma_\parallel A_\parallel(\text{flux}) \ , \tag{B.3}$$

$$P_T = Q_\parallel A_\parallel(\text{power}) \ . \tag{B.4}$$

Here $A_\parallel$ is the effective total module area perpendicular to the flow. For a limiter system with full flux coverage, $N > N_{ff}$, we have shadowing between the modules. As shown in Fig. 6(a), if we assume, for example, $N_s = 3$ modules that partially shadow each other, then

$$A_\parallel(\text{flux}) = 2N(w_1\lambda_1 + 2w_2\lambda_2) \ ,$$

where $L_\theta = w_1 + 2w_2$, $\lambda_j \equiv \lambda_\Gamma(j)$, and $\lambda_2 = \lambda_1/\sqrt{2}$. Using $\alpha_s = w_1/L_\theta$ for the nonshadowed poloidal extent of the module in this equation, we find

$$A_\parallel(\text{flux}) = 2NL_\theta\lambda_\Gamma(\text{NS})[\alpha_s + (1-\alpha_s)/\sqrt{2}] \ , \tag{B.5}$$

where $\lambda_\Gamma(\text{NS})$ is the particle flux scale length if the module is nonshadowed.

Similarly, for the power flux we have

$$A_\parallel(\text{power}) = A_\parallel(\text{flux})[\lambda_q(\text{NS})/\lambda_\Gamma(\text{NS})] \ , \tag{B.6}$$

where $\lambda_q(\text{NS})$ is the heat flux scale length for a nonshadowed module.

From these relations, we find the SOL boundary ($x = 0$) fluxes to be:

$$\Gamma_0 = \frac{N_e/\bar{\tau}_p}{2NL_\theta\lambda_\Gamma[\alpha_s + (1-\alpha_s)/\sqrt{2}]} ,$$

$$\frac{Q_0}{\Gamma_0} = \frac{P_T}{N_e/\bar{\tau}_p}\left(\frac{\lambda_\Gamma}{\lambda_q}\right) , \tag{B.7}$$

where $\alpha_s = w_1/L_\theta = 2N_{ff}/N - 1$, as discussed in Section III [Eq. (47)]. Using this, we obtain

$$\Gamma_0 = \frac{N_e/\bar{\tau}_p}{2NL_\theta\lambda_\Gamma(C_1 + C_2\ N_{ff}/N)} , \tag{B.8}$$

with $C_1 = \sqrt{2}-1$, $C_1 + C_2 = 1$. We also have $N_{ff}L_\theta = 2\pi a/q$ in these relationships. Equation (B.7) is also related to

$$Q_0 = \gamma\Gamma_0 T_e , \tag{B.9}$$

where γ is the heat transmission coefficient, which is given by[21]

$$\gamma = 2\frac{T_i}{T_e} + \frac{2}{1-\gamma_s} - 0.5\ln\left[\left(2\pi\frac{m_e}{m_i}\right)\left(1+\frac{T_i}{T_e}\right)\Big/(1-\gamma_s)^2\right] , \tag{B.10}$$

with γ_s the secondary electron emission coefficient.

We now apply these results to Tore Supra and estimate the SOL boundary ($x = 0$) parameters, such as Γ_0, T_e, n_e, and λ_n. We have $P_T \simeq 6$ MW and $N_e/\bar{\tau}_p \simeq 2 \times 10^{22}$ s^{-1}, $a = 0.75$ m, $R_0 = 2.4$ m, $q(a) = 3$, and $N = 6$ modules. Using $\lambda_\Gamma/\lambda_q = 7/5$ and taking[21] $\gamma \simeq 10$ for $\gamma_s \simeq 0.6$, from Eqs. (B.7) and (B.9) we first estimate

$$T_e \simeq 260 \text{ eV} , \tag{B.11}$$

and for the Bohm diffusion coefficient

$$D_\perp(\text{cm}^2/\text{s}) \simeq (6.25 \times 10^2) \times T_e(\text{eV})/B(\text{T}) \simeq 3.6 \times 10^4 \text{cm}^2/\text{s} \tag{B.12}$$

for $B \simeq 4.5$ T.

The connection length for a nonshadowed module $L_c \simeq 2.2 \times 10^3$ cm, and from the parallel flow loss time $\tau_{\|} \simeq 2.8 \times 10^{-4}$ s for hydrogen plasmas. By combining these results in Eq. (B.2), we obtain $\lambda_n(\text{NS}) \simeq 3.2$ cm.

The value of the particle flux at $x = 0$, from Eq. (B.8), is

$$\Gamma_0 \simeq 3 \times 10^{19} \text{ cm}^{-2}/\text{s} .$$

Here we have used $N_{\rm ff} = 4$ for $L_\theta = 40$ cm; that corresponds to $\alpha_s \simeq 0.33$ for the fraction of the nonshadowed module poloidal extent, as we observe from Fig. 8. The plasma density is readily obtained from $\Gamma_0 = n_e v_{\|}$, and we find that $n_e(x = 0) \simeq 4 \times 10^{12}$ cm^{-3}.

ORNL/TM-10164
Dist. Category UC-20 a,d,f

INTERNAL DISTRIBUTION

1. F. W. Baity
2. L. A. Berry
3. R. E. Clausing
4. J. L. Dunlap
5. R. D. Foskett
6. D. L. Hillis
7–11. C. C. Klepper
12. R. A. Langley
13. J. F. Lyon
14–18. P. K. Mioduszewski
19. M. Murakami
20. J. Sheffield
21. J. E. Simpkins
22. N. A. Uckan
23–27. T. Uckan
28–29. Laboratory Records Department
30. Laboratory Records, ORNL-RC
31. Document Reference Section
32. Central Research Library
33. Fusion Energy Division Library
34–35. Fusion Energy Division Publications Office
36. ORNL Patent Office

EXTERNAL DISTRIBUTION

37. Office of the Assistant Manager for Energy Research and Development, U.S. Department of Energy, Oak Ridge Operations Office, P. O. Box E, Oak Ridge, TN 37831
38. J. D. Callen, Department of Nuclear Engineering, University of Wisconsin, Madison, WI 53706-1687
39. J. F. Clarke, Director, Office of Fusion Energy, Office of Energy Research, ER-50 Germantown, U.S. Department of Energy, Washington, DC 20545
40. R. W. Conn, Department of Chemical, Nuclear, and Thermal Engineering, University of California, Los Angeles, CA 90024
41. S. O. Dean, Fusion Power Associates, 2 Professional Drive, Suite 248, Gaithersburg, MD 20879
42. H. K. Forsen, Bechtel Group, Inc., Research Engineering, P. O. Box 3965, San Francisco, CA 94105
43. J. R. Gilleland, GA Technologies, Inc., Fusion and Advanced Technology, P.O. Box 81608, San Diego, CA 92138
44. R. W. Gould, Department of Applied Physics, California Institute of Technology, Pasadena, CA 91125
45. R. A. Gross, Plasma Research Laboratory, Columbia University, New York, NY 10027
46. D. M. Meade, Princeton Plasma Physics Laboratory, P.O. Box 451, Princeton, NJ 08544

47. M. Roberts, International Programs, Office of Fusion Energy, Office of Energy Research, ER-52 Germantown, U.S. Department of Energy, Washington, DC 20545
48. W. M. Stacey, School of Nuclear Engineering and Health Physics, Georgia Institute of Technology, Atlanta, GA 30332
49. D. Steiner, Nuclear Engineering Department, NES Building, Tibbetts Avenue, Rensselaer Polytechnic Institute, Troy, NY 12181
50. R. Varma, Physical Research Laboratory, Navrangpura, Ahmedabad 380009, India
51. Bibliothek, Max-Planck Institut fur Plasmaphysik, D-8046 Garching, Federal Republic of Germany
52. Bibliothek, Institut fur Plasmaphysik, KFA, Postfach 1913, D-5170 Julich, Federal Republic of Germany
53. Bibliotheque, Centre des Recherches en Physique des Plasmas, 21 Avenue des Bains, 1007 Lausanne, Switzerland
54. F. Prevot, CEN/Cadarache, Departement de Recherches sur la Fusion Controlee, F-13108 Saint-Paul-lez-Durance Cedex, France
55. Documentation S.I.G.N., Departement de la Physique du Plasma et de la Fusion Controlee, Centre d'Etudes Nucleaires, B.P. 85, Centre du Tri, F-38041 Grenoble, France
56. Library, Culham Laboratory, UKAEA, Abingdon, Oxfordshire, OX14 3DB, England
57. Library, FOM-Instituut voor Plasma-Fysica, Rijnhuizen, Edisonbaan 14, 3439 MN Nieuwegein, The Netherlands
58. Library, Institute of Plasma Physics, Nagoya University, Nagoya 464, Japan
59. Library, International Centre for Theoretical Physics, P.O. Box 586, I-34100 Trieste, Italy
60. Library, Laboratorio Gas Ionizatti, CP 56, I-00044 Frascati, Rome, Italy
61. Library, Plasma Physics Laboratory, Kyoto University, Gokasho, Uji, Kyoto, Japan
62. Plasma Research Laboratory, Australian National University, P.O. Box 4, Canberra, A.C.T. 2000, Australia
63. Thermonuclear Library, Japan Atomic Energy Research Institute, Tokai Establishment, Tokai-mura, Naka-gun, Ibaraki-ken, Japan
64. G. A. Eliseev, I. V. Kurchatov Institute of Atomic Energy, P. O. Box 3402, 123182 Moscow, U.S.S.R.
65. V. A. Glukhikh, Scientific-Research Institute of Electro-Physical Apparatus, 188631 Leningrad, U.S.S.R.
66. I. Shpigel, Institute of General Physics, U.S.S.R. Academy of Sciences, Ulitsa Vavilova 38, Moscow, U.S.S.R.
67. D. D. Ryutov, Institute of Nuclear Physics, Siberian Branch of the Academy of Sciences of the U.S.S.R., Sovetskaya St. 5, 630090 Novosibirsk, U.S.S.R.

68. V. T. Tolok, Kharkov Physical-Technical Institute, Academical St. 1, 310108 Kharkov, U.S.S.R.
69. Library, Academia Sinica, P.O. Box 3908, Beijing, China (PRC)
70. R. A. Blanken, Experimental Plasma Research Branch, Division of Applied Plasma Physics, Office of Fusion Energy, Office of Energy Research, ER-542 Germantown, U.S. Department of Energy, Washington, DC 20545
71. K. Bol, Princeton Plasma Physics Laboratory, P.O. Box 451, Princeton, NJ 08544
72. R. A. E. Bolton, IREQ Hydro-Quebec Research Institute, 1800 Montee Ste.-Julie, Varennes, P.Q. JOL 2P0, Canada
73. D. H. Crandall, Experimental Plasma Research Branch, Division of Applied Plasma Physics, Office of Fusion Energy, Office of Energy Research, ER-542 Germantown, U.S. Department of Energy, Washington, DC 20545
74. R. L. Freeman, GA Technologies, Inc., P.O. Box 81608, San Diego, CA 92138
75. K. W. Gentle, RLM 11.222, Institute for Fusion Studies, University of Texas, Austin, TX 78712
76. R. J. Goldston, Princeton Plasma Physics Laboratory, P.O. Box 451, Princeton, NJ 08544
77. J. C. Hosea, Princeton Plasma Physics Laboratory, P.O. Box 451, Princeton, NJ 08544
78. S. W. Luke, Division of Confinement Systems, Office of Fusion Energy, Office of Energy Research, ER-55 Germantown, U.S. Department of Energy, Washington, DC 20545
79. E. Oktay, Division of Confinement Systems, Office of Fusion Energy, Office of Energy Research, ER-55 Germantown, U.S. Department of Energy, Washington, DC 20545
80. D. Overskei, GA Technologies, Inc., P.O. Box 81608, San Diego, CA 92138
81. R. R. Parker, Plasma Fusion Center, NW 16-288, Massachusetts Institute of Technology, Cambridge, MA 02139
82. W. L. Sadowski, Fusion Theory and Computer Services Branch, Division of Applied Plasma Physics, Office of Fusion Energy, Office of Energy Research, ER-541 Germantown, U.S. Department of Energy, Washington, DC 20545
83. J. W. Willis, Division of Confinement Systems, Office of Fusion Energy, Office of Energy Research, ER-55 Germantown, U.S. Department of Energy, Washington, DC 20545
84. A. P. Navarro, Division de Fusion, Junta de Energia Nuclear, Avenida Complutense 22, E-28040 Madrid, Spain
85. Laboratory for Plasma and Fusion Studies, Department of Nuclear Engineering, Seoul National University, Shinrim-dong, Gwanak-ku, Seoul 151, Korea
86. R. T. McGrath, Sandia National Laboratories, Albuquerque, NM 87175
87. J. B. Whitley, Sandia National Laboratories, Albuquerque, NM 87175

88. R. Aymar, Centre d'Etudes Nucléaires de Cadarache, B.P. No. A1, 13108 Saint Paul-lez-Durance Cedex, France
89. R. Deschamps, Centre d'Etudes Nucléaires de Cadarache, B.P. No. A1, 13108 Saint Paul-lez-Durance Cedex, France
90. R. Gravier, Centre d'Etudes Nucléaires de Cadarache, B.P. No. A1, 13108 Saint Paul-lez-Durance Cedex, France
91. D. Grossman, Centre d'Etudes Nucléaires de Cadarache, B.P. No. A1, 13108 Saint Paul-lez-Durance Cedex, France
92. D. Markevich, Advanced Fusion Concepts Branch, Division of Applied Plasma Physics, Office of Fusion Energy, Office of Energy Research, ER-543 Germantown, U.S. Department of Energy, Washington, DC 20545
93. K. H. Dippel, KFA Jülich, Postfach 1913, D-5170 Jülich 1, Federal Republic of Germany

94–238. Given distribution according to TIC-4500, Magnetic Fusion Energy (Category UC-20 a, d, f,: Plasma Systems, Fusion Systems, Experimental Plasma Physics)